

PERFORMANCE ANALYSIS OF DIFFERENT PULSE COMPRESSION TECHNIQUES FOR IMPROVING RANGE RESOLUTION IN RADAR TECHNOLOGY

A thesis submitted in partial fulfillment of the requirements for the degree of

**Bachelor of Science
in
Electrical Electronic and Communication Engineering**

Submitted by

**Md. Tanjilul Alam
Md. Roman Sarker
Md. Maynul Islam**

**Student ID No. : 201016057
Student ID No. : 201016062
Student ID No. : 201016063**

Under the Supervision of
Gp Capt Dr. Mohammed Hossam-E-Haider



Department of Electrical Electronic and Communication Engineering
Military Institute of Science and Technology
December, 2013

CERTIFICATION

This thesis paper titled “**PERFORMANCE ANALYSIS OF DIFFERENT PULSE COMPRESSION TECHNIQUES FOR IMPROVING RANGE RESOLUTION IN RADAR TECHNOLOGY**” is submitted by the group as mentioned below has been accepted as satisfactory in partial fulfillment of the requirements for the degree of B Sc in Electrical Electronic and Communication Engineering on December 2013.

Group Members:

Md. Tanjilul Alam

Md. Roman Sarker

Md. Maynul Islam

SUPERVISOR:

Gp Capt Dr. Mohammed Hossam-E-Haider

Senior Instructor

Department of Electrical, Electronic and Communication Engineering (EECE)

Military Institute of Science and Technology (MIST)

Mirpur Cantonment, Dhaka-1216.

DECLARATION

It is hereby declared that the work presented in the thesis titled “**PERFORMANCE ANALYSIS OF DIFFERENT PULSE COMPRESSION TECHNIQUES FOR IMPROVING RANGE RESOLUTION IN RADAR TECHNOLOGY**” is an outcome of the study carried out by the author under the supervision of Gp Capt Dr. Mohammed Hossam-E-Haider. It is also declared that neither of this thesis paper nor any part therefore has been submitted anywhere else for the award of any degree, diploma or other qualifications.

AUTHORS:

Md. Tanjilul Alam

Student ID No.: 2010160657

Md. Roman Sarker

Student ID No.: 201016062

Md. Maynul Islam

Student ID No.: 201016063

ACKNOWLEDGEMENT

We are thankful to Almighty Allah for giving us the course and enthusiasm to complete the thesis work. Our heartiest gratitude, profound indebtedness and deep respect go to our supervisor Gp Capt Dr. Md Hossam-E-Haider, Senior Instructor, Department of Electrical, Electronic and Communication Engineering (EECE), Military Institute of Science and Technology (MIST), Dhaka, Bangladesh, for his constant supervision, affectionate guidance and great encouragement and motivation. His keen interest on the topic and valuable advices throughout the study was of great help in completing our thesis work.

Dhaka

December 2013

Md. Tanjilul Alam

Md.Roman Sarker

Md. Maynul Islam

ABSTRACT

RADAR, which is an abbreviation for Radio Detection And Ranging, is an electromagnetic system for the detection and location of reflecting objects such as aircraft, ships, spacecraft, vehicles, people and natural environment. Detectability of an object or target depends on range resolution of reflected signal from the object or target. The range resolution of Radar is defined as the minimum separation (in range) of two targets or equal cross section that can be resolved as separate targets. It is determined by the bandwidth of the reflected signal. As spectral bandwidth of a pulse is inversely proportional to its width, the bandwidth of a short pulse is large. Range resolution for given radar can be significantly improved by using very short pulses. As short pulses decreases the average transmitted power, pulse compression allows us to achieve the average transmitted power of a relatively long pulse, while obtaining the range resolution corresponding to a short pulse.

Pulse compression technique is generally used in Radar system in order to improve the target detection and range resolution. A Problem arises in pulse compression technique because of masking of small targets by the range side lobes of large nearby targets. Another problem is for multiple targets-main lobes of the compressed pulses overlap each other.

This thesis has proposed a technique to suppress the side lobes and eradicate the problem of overlapping by comparing different pulse compression techniques. In the simulation, we compared the result of analog pulse compression output by applying different weighting function. For multiple targets we compare the output of stretch processor technique with Barker Codes of different lengths. It is revealed that Barker Code of length thirteen (B_{13}) is better both for reduction of side lobes and detecting multiple targets.

TABLE OF CONTENTS

CERTIFICATION	ii
DECLARATION	iii
ACKNOWLEDGEMENT	iv
ABSTRACT	v
TABLE OF CONTENTS	vi
LIST OF FIGURES	ix
LIST OF ABBREVIATION	xii
CHAPTER 1 INTRODUCTION	1
1.1. Radar Fundamentals	1
1.1.1. Definition and Basic Function	1
1.1.2. Basic Radar Block Diagram	2
1.1.3. Classification of Radar	4
1.2. Continuous Wave (CW) and Pulsed Radars	6
1.2.1. CW Radar	6
1.2.2. Pulsed Radar	7
1.3. Radar Terminologies	8
1.3.1. PRF.....	8
1.3.2. Maximum Unambiguous Range	9
1.3.3. Range Resolution (ΔR)	9
1.3.4. Doppler Shift	11
1.3.5. Coherence	13
1.4. Objective of the Thesis	13
1.5. Organization of the Thesis	14

CHAPTER 2 RADAR EQUATIONS AND PARAMETERS	15
2.1. Basic Radar Equation	15
2.1.1. Mono-static Radar Equation.....	15
2.1.2. Noiseless Case	15
2.1.3. With the Presence of Noise	16
2.2. Variations of Basic Equation	18
2.2.1. Bistatic Radar Equation.....	18
2.2.2. Low PRF Radar Equation.....	19
2.2.3. High PRF Radar Equation	20
CHAPTER 3 PULSE COMPRESSION FUNDAMENTALS	21
3.1. Matched Filter	21
3.1.1. Matched Filter Replica	22
3.2. The Radar Ambiguity Function	24
3.2.1. Properties of Radar Ambiguity Function	25
3.3. Correlation	26
3.3.1. To use correlation	27
3.3.2. Cross-correlation.....	27
3.3.2.1. Properties	28
3.3.3. Auto-correlation.....	29
3.3.3.1. Properties	30
3.4. Weighting Functions	32
3.4.1. Rectangular Window.....	33
3.4.1.1. Properties	34
3.4.2. Kaiser Window	35
3.4.3. Hamming Window.....	37
3.4.4. Chebyshev Window	38

CHAPTER 4 PULSE COMPRESSION	39
4.1. Definition	39
4.2. Time-Bandwidth Product.....	40
4.3. Radar Equation with Pulse Compression	41
4.4. Analog Pulse Compression	42
4.4.1. Correlation Processor	43
4.4.2. Stretch Processor.....	48
4.4.3. Distortion Due to Target Velocity	52
4.5. Digital Pulse Compression.....	54
4.5.1. Frequency Coding (Costas Codes).....	54
4.5.2. Binary Phase Code	56
4.5.3. Frank Codes	60
4.5.4. Pseudo-Random (PRN) Codes	62
Chapter 5 COMPERATIVE STUDY AMONG DIFFERENT PULSE COMPRESSION TECHNIQUES	65
5.1. Introduction.....	65
5.2. Simulation of Different Pulse compression	65
5.2.1. Pulse compression Using Matched Filter	66
5.2.1.1. Window Variation over matched filter response.....	68
5.2.2. Stretch Processor.....	70
5.2.3 Digital Pulse Compression	72
5.3. Result and Discussion on Simulation	74
CHAPTER 6 CONCLUTION AND FUTURE WORKS	75
6.1. Results and Discussions.....	75
6.2. Scope of Future Works	77
BIBLIOGRAPHY	78
APPENDIX	79

LIST OF FIGURES

Figure 1.1. Radar Block Diagram.....	3
Figure 1.2. Pulse radar in operation.....	7
Figure 1.3. PRF and IPP	8
Figure 1.4. Range resolutions (a) Two unresolved targets, (b) Two resolved targets.....	10
Figure 1.5. Effect of target motion on the reflected equiphase waveforms	11
Figure 1.6. Doppler shift due to moving radar and targets.....	11
Figure 1.7. Phase continuity between consecutive pulses.	13
Figure 2.1. Bistatic radar geometry	18
Figure 3.1. A block diagram of Pulse Compression based on FFT and Inverse FFT.	23
Figure 3.2. Comparison between the ultimate resolution of rectangular constant frequency pulse and a chirp pulse of the same duration.....	24
Figure 3.3. Cross correlation showing two targets with different amplitudes and at different ranges: BPSK radar noise sequence generated using a 12bit shift register with 4096 points	31
Figure 3.4. Cross correlation showing two targets with different amplitudes and at different ranges: BPSK radar noise sequence generated using a 12bit shift register with 4095 points	32
Figure 3.5. Rectangular Window.....	34
Figure 3.6. Kaiser Window	36
Figure 3.7. Hamming Window.....	37
Figure 3.8. Chebyshev Window.....	38
Figure 4.1. Input noise power.....	40
Figure 4.2. (a) Composite echo signal for two unresolved targets.....	43
Figure 4.2. (b) Composite echo signal corresponding to Fig. 4.2a, after pulse compression.....	44
Figure 4.3. Computing the matched filter output using an FFT.....	45
Figure 4.4. Reducing the first side lobe to -42 dB doubles the main lobe width	46
Figure 4.5. Uncompressed echo signal. Scatterers are unresolve.....	47

Figure 4.6. Compressed echo signal. Scatterers are resolve.....	47
Figure 4.7. Stretch Processor Block Diagram.....	50
Figure 4.8. Uncompressed echo signal. 3 targets are unresolved.....	51
Figure 4.9. Compressed echo signal. 3 targets are resolved	51
Figure 4.10. (a) Compressed pulse output of a pulse compression processor. No distortion is present.....	52
Figure 4.10. (b) Mismatched compressed pulse; 5% Doppler shift.	53
Figure 4.10. (c) Mismatched compressed pulse; 10% time dilation	53
Figure 4.11. Frequency assignment for a burst of N sub pulses. (a) SFW (stepped LFM);(b)Costas code of length $N_c = 10$	55
Figure 4.12. Binary phase code of length 7.....	57
Figure 4.13. Binary phase code of length 13.....	59
Figure 4.14. Binary phase code of length 15.....	60
Figure 4.15. A linear transversal filter of order N can be used to produce N zero side lobes in the autocorrelation function. In this figure, $N = 4$	60
Figure 4.16. Stepwise approximation of an up-chirp waveform.....	62
using a Frank code of 16 elements.	62
Figure 4.17. Typical correlation of an MLS code of length L.....	63
Figure 4.18. Circuit for generating an MLS sequence of length $L = 15$	64
The primitive polynomial is $x^4 + x + 1$	64
Figure 5.1. Uncompressed Echo of Received Signal	66
Figure 5.2. Matched filter time domain response.....	67
Figure 5.3. Matched frequency domain response.....	67
Figure 5.4. Compressed echo of received signal using no weighting function.....	68
Figure 5.5. (a) Compressed echo of received signal using hamming weighting function.....	69
Figure 5.5. (b) Compressed echo of received signal using Kaiser weighting function...	69
Figure 5.5. (c) Compressed echo of received signal using chebyshev weighting function.....	70
Figure 5.6. (a) Compressed echo for single target using stretch processing technique...	71
Figure 5.6. (b) Compressed echo for two targets using stretch processing technique.....	71
Figure 5.6. (c) Compressed echo for three targets using stretch processing technique...	72

Figure 5.7. (a) Digital pulse compression technique using Barker Code of length Three (**B3**) for three targets 73

Figure 5.7. (b) Digital pulse compression technique using Barker Code of length Seven (**B7**) for three targets 73

Figure 5.7. (c) Digital pulse compression technique using Barker Code of length Thirteen (**B13**) for three targets..... 73

LIST OF ABBREVIATION

CW	-	Continuous Wave
FCP	-	Fast Convolution Processing
FMCW	-	Frequency Modulated Continuous Wave
HRR	-	High Range Resolution
IPP	-	Inter Pulse Period
LFM	-	Linear Frequency Modulation
LTI	-	Linear Time Invariant
MLS	-	Maximal Length Sequences
MTI	-	Moving Target Indication
NBF	-	Narrow Band Filters
PRI	-	Pulse Repetition Frequency
PRF	-	Pulse Repetition Frequency
PRN	-	Pseudo-Random
PSD	-	Pulse Spectral Density
RADAR	-	Radio Detection And Ranging
RCS	-	Radar Cross Section
SAW	-	Surface Acoustic Wave
SNR	-	Signal to Noise Ratio
SFW	-	Stepped Frequency Waveform

Chapter 1

INTRODUCTION

1.1. Radar Fundamentals

1.1.1. Definition and Basic Function

The word RADAR is an abbreviation for Radio Detection And Ranging. Radar is an electromagnetic system for the detection and location of reflecting objects such as aircraft, ships, spacecraft, vehicles, people and the natural environment. In general, radar systems use modulated waveforms and directive antennas to transmit electromagnetic energy into a specific volume in space to search for targets. Objects (targets) within a search volume will reflect portions of this energy (radar returns or echoes) back to the radar. This small echo signal along with noise is processed by high sensitivity signal processor to determine the exact location, range, velocity, angular position, size and other target identifying information varying according to the type of radar used. Radar can be used to detect aircraft, ships, spacecraft, guided missiles, motor vehicles, weather formations, and terrain. The modern uses of radar are highly diverse, including air traffic control, radar astronomy, air-defense systems, antimissile systems, marine radars to locate landmarks and other ships; aircraft anti-collision system, ocean surveillance system, outer space surveillance and rendezvous systems, meteorological precipitation monitoring, altimetry and flight control systems; guided missile target locating systems; and ground-penetrating radar for geological observations. High tech radar systems are associated with digital signal processing and are capable of extracting useful information from very high noise levels. There are no competitive techniques that can accurately measure long ranges in both clear and adverse weather as well as can radar.

Conventional radars operate using radio waves or microwaves. Radar can also make use of other parts of the electromagnetic spectrum.

The most important functions that radar can perform are

- Resolution
- Detection
- Measurement
- Tracking

Resolution corresponds to radar's ability to resolve (separate) one target signal from another. Larger bandwidths give better resolution in the range parameter, while long transmitted pulses give better resolution in frequency.

Detection function is the ability of the radar to be able to sense the presence of the reflected target signal in the radar receiver. The function is complicated by the unwanted reflected signal (clutter) and the receiver noise.

- Noise is reduced by better receiver design and transmitting signals with larger energy per pulse.
- Clutter is reduced by proper signal design and appropriate signal-processing methods.

Measure function is radar's ability to measure a target's position in 3-D space, its velocity vector, angular direction, and vector angular velocity. Advanced radars even can measure target extent (size), shape, and classification (truck, tank etc.). With the advancement of technology classification of target may become the fourth most important function of radar. **Tracking** function enables radar not only to recognize the presence of a target but to determine the target's location in range and in one or two angle coordinates. As it continues to observe a target over time, the radar can provide the target's trajectory, or track and predict where it will be in the future.

1.1.2. Basic Radar Block Diagram

A simplified pulsed radar block diagram is illustrated in Fig. 1.1. This shows a Radar

where the transmitter and the receiver are in same place.

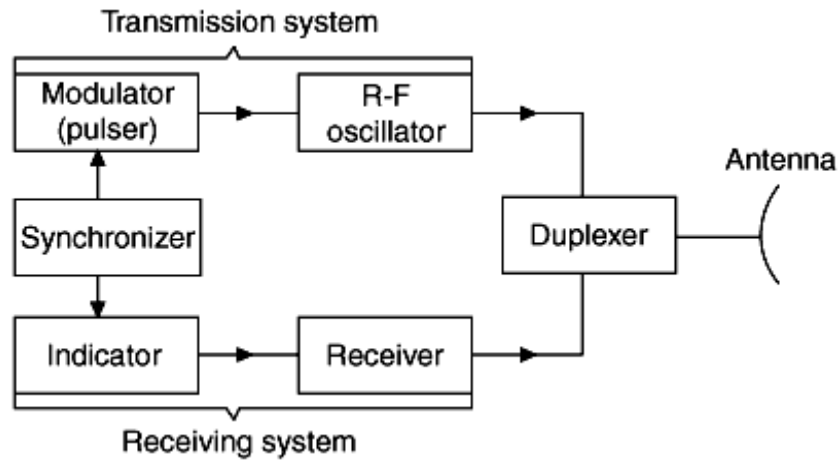


Figure 1.1. Radar Block Diagram

A modulated signal is generated and sent to the antenna by the modulator/transmitter block. Switching the antenna between the transmitting and receiving modes is controlled by the duplexer. The duplexer allows one antenna to be used to both transmit and receive. During transmission it directs the radar electromagnetic energy towards the antenna. Alternatively, on reception, it directs the received radar echoes to the receiver. The receiver amplifies the radar returns and prepares them for signal processing. Extraction of target information is performed by the signal processor block. The target's range, R , is computed by measuring the time delay Δt ; it takes a pulse to travel the two-way path between the radar and the target. Since electromagnetic waves travel at the speed of light, $c = 3 \times 10^8$ m/s, then

$$R = \frac{c\Delta t}{\tau} \tag{1.1}$$

Where R is in meters and Δt is in seconds.

1.1.3. Classification of Radar

Radar systems have different qualities and technologies. There are many points for radar Classifications.

A- The Separation Between Tx and Rx

- **Monostatic Radar:** Both transmitter and receiver in the same location.
- **Bistatic Radar:** The transmitter and receiver are placed in different locations.
- **Multistatic Radar:** There are one transmitter and several receivers placed in different locations

B- Installation or Location:

- **Ground based radar:**

This type of radar is characterized by:

- a) Very large antenna.
- b) Great size and weight.
- c) Long detection range.
- d) Used as long range surveillance radar.

- **Naval Radars:** They are used as navigation aids and safety device to locate buoys, shore lines, and other ships.
- **Airborne Radars:** They are usually used on aircrafts so they have as possible as small size and weight, they are used in navigation, terrain following and avoidance, weather warning radar and surface mapping radar.
- **Space Based Radars:** They may be used to assist in guidance of spacecraft and for remote sensing of the land and sea.

C- Measured Coordinates

- **One Dimensional (1-D) Radar:** (Range finder measures the range) or (Altimeter measures the height).
- **Two Dimensional (2-D) Radar:** measures both range and azimuth.
- **Three Dimensional (3-D) Radar:** measures range, azimuth and elevation.

D- Transmission Waveform

- **Continuous Wave (CW) Radar**

It is based on transmission of CW radio frequency energy. When CW energy is reflected from moving target, the return is Doppler shifted. It is used as speed traps and speed meters. It is inexpensive short ranges systems but in long range systems it becomes difficult to separate between transmitter and receiver operation.

- **Frequency Modulated Continuous Wave (FMCW)**

CW radar cannot indicate target range. One way to solve the problem is to modulate the transmitter output frequency. A triangular or sinusoidal modulating wave form is commonly used by measuring the difference of frequency between the instantaneous transmitter frequency and the frequency of the received echo. Thus it is possible to obtain the range of the target.

- **Pulsed Radar:**

Electromagnetic energy is transmitted as a series of pulses. Target range is found by measuring the time for echoes to return to the receiver. There are several forms of pulse radar such as:

- a) **MTI (Moving Target Indication):** This radar is developed for discrimination in favor of aircraft and other moving target.

- b) **Pulse Doppler Radar:** The difference between MTI and pulse doppler radar is that MTI uses PRF low enough to avoid range ambiguity, while pulse doppler radar avoids velocity ambiguity using higher PRF. In Practice MTI pulse radar is more common.

E- Type of Processing:

- Coherent.
- MTI and Pulse Doppler.
- Non coherent.
- Phased Array Radar.

1.2. Continuous Wave (CW) and Pulsed Radars

1.2.1. CW Radar

Continuous wave radar systems are those which use a stable frequency continuous wave for transmission and reception. CW radars depend on the doppler frequency shift of the echo signal, caused by a moving target, to separate in the frequency domain the weak echo signal from the large transmitted signal and the echoes from fixed clutter (land, sea or weather), as well as to measure the radial velocity of the target. This doppler shift is related to the target velocity by the relation:

$$f_D = \frac{2V_r}{\lambda} \quad (1.2)$$

The main advantages of the CW radars are:

- Simple to manufacture.
- No minimum or maximum range (broadcast power level imposes a practical limit on range).
- Maximize power on a target due to continuous broadcasting.

However they also have the following disadvantages:

- They can only detect moving targets, as stationary targets (along the line of sight) will not cause a Doppler shift.
- They cannot measure range. Range is normally measured by timing the delay between a pulse being sent and received, but as CW radars are always broadcasting, there is no delay to measure. Ranging can be implemented, however, by use of a technique known as frequency modulated continuous-wave radar.

1.2.2. Pulsed Radar

Pulsed Radars use a train of pulsed waveforms with modulation. Basing on pulse repetition frequency or PRF (definition given in the next section), Pulsed radars are classified as low PRF, medium PRF and High PRF. Low PRF radars are used primarily for ranging where target velocity is not needed. High PRF radars are used for measuring target velocity (Doppler Shift).

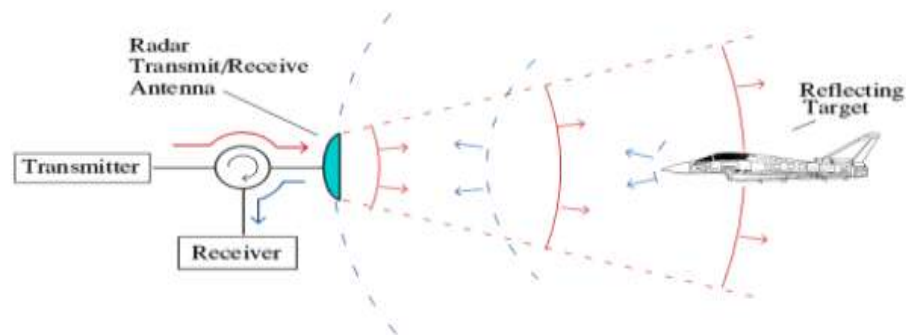


Figure 1.2. Pulse radar in operation.

One of pulse radar advantages is that the transmitter is turned off most of the time. The receiver can listen for returning echoes without any interference from the transmitter. Pulsed radars which extract the doppler frequency shift are called either moving target indication (MTI) or pulse doppler radars depending on their particular values of pulse repetition frequency and duty cycle. MTI radar has a low PRF and a low duty cycle. A

pulse doppler radar on the other hand has a high PRF and a high duty cycle.

1.3. Radar Terminologies

1.3.1. PRF

Pulsed radar uses a train of pulse for transmission and reception as illustrated Fig. 1.3. The time interval between any two transmitted pulses is known as the Pulse Repetition Interval (PRI) or Inter Pulse Period (IPP) denoted by T . The inverse of PRI is called Pulse Repetition Frequency (PRF) denoted by f_r . During each PRI radar radiates energy only for τ (pulse width) seconds and listens for target returns for rest of the PRI. Here

$$F_r = \frac{1}{PRI} = \frac{1}{T} \quad (1.3)$$

Radar transmitting duty cycle is

$$d_t = \frac{\tau}{T} \quad (1.4)$$

And the radar average transmitted power is

$$P_{avg} = P_t * d_t \quad (1.5)$$

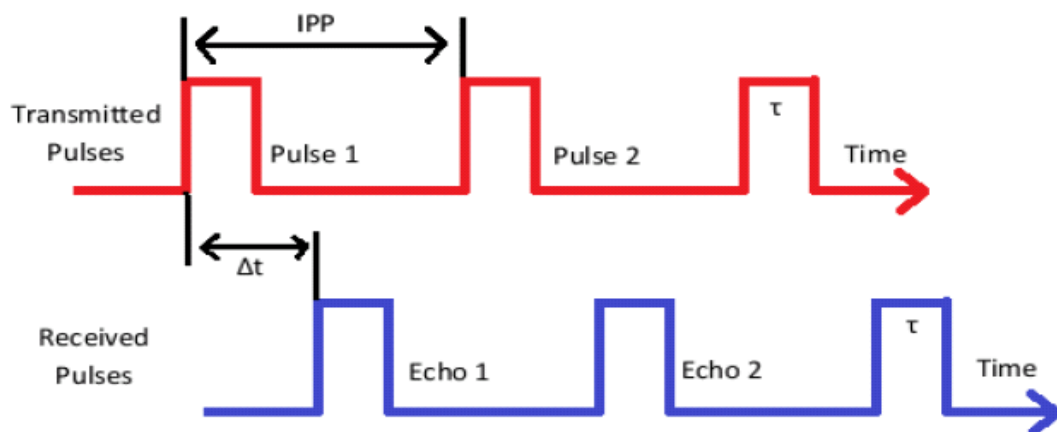


Figure 1.3. PRF and IPP.

From the above equations it is clear that increasing the pulse width means increasing the transmitting duty cycle which in turn increases the radar average transmitted power thereby increasing the SNR.

1.3.2. Maximum Unambiguous Range

Once a pulse is transmitted sufficient time must elapse to allow all echo signals to return to the radar before the next pulse is transmitted. The rate at which pulses may be transmitted, therefore, is determined by the longest range at which targets are expected. If the time between pulses T_p is too short an echo signal from a long-range target might arrive after the transmission of the next pulse and be mistakenly associated with that pulse rather than the actual pulse transmitted earlier. This can result in an incorrect or ambiguous measurement of the range. The range beyond which targets appear as second-time around echoes is the maximum unambiguous range, R_u and is given by

$$R_u = \frac{cT}{2} \quad (1.6)$$

Where T_p = pulse repetition period = $1/f_p$ and f_p = pulse repetition frequency (prf).
Therefore the maximum unambiguous range (R_u) corresponds to half of PRI.

1.3.3. Range Resolution (ΔR)

It is the radar's ability to detect targets in close proximity to each other as distinct objects. Radars have a minimum range R_{mn} and a maximum range R_{mx} . The whole range area is divided into number of range bins or gates (M) each of width ΔR . Targets separated by at least ΔR can be completely resolved in range. Targets within the same range bin can be resolved in cross range (horizontally) utilizing signal processing techniques. To find the minimum ΔR let us assume two targets separated by $\frac{c\tau}{4}$ as shown in Fig. 1.4(a). In this case, when the pulse trailing edge strikes target 2 the leading-edge would have traveled backwards a distance $c\tau$ and the returned pulse would

be composed of returns from both targets (i.e., unresolved return).

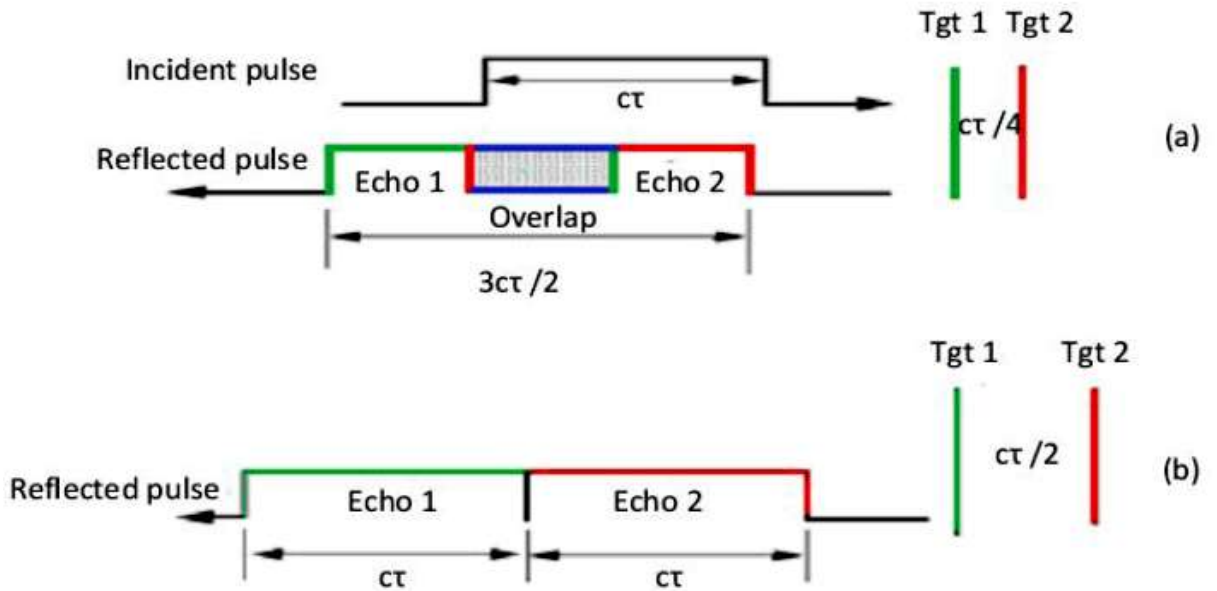


Figure 1.4. Range resolutions (a) Two unresolved targets, (b) Two resolved targets.

However, if the two targets are at least $c\tau/2$ apart, then as the pulse trailing edge strikes the first target the leading edge will start to return from target 2, and two distinct returned pulses will be produced, as illustrated by Fig. 1.4(b). Thus, ΔR should be greater or equal to $c\tau/2$. And since the radar bandwidth B is equal to $1/\tau$, then

$$\Delta R = \frac{c\tau}{2} = \frac{c}{2B} \quad (1.7)$$

In general, radar users and designers alike seek to minimize in order to enhance the radar performance. As suggested by Eq. 1.5, in order to achieve fine range resolution one must minimize the pulse width. However, this will reduce the average transmitted power and increase the operating bandwidth. Achieving fine range resolution while maintaining adequate average transmitted power can be accomplished by using pulse compression techniques.

1.3.4. Doppler Shift

Doppler shift is an apparent change in frequency (or wavelength) due to the relative motion of two objects. When the two objects are approaching each other, the doppler shift causes a shortening of wavelength or increase in frequency. When the two objects are moving away from each other, the doppler shift causes a lengthening of wavelength or decrease in frequency.

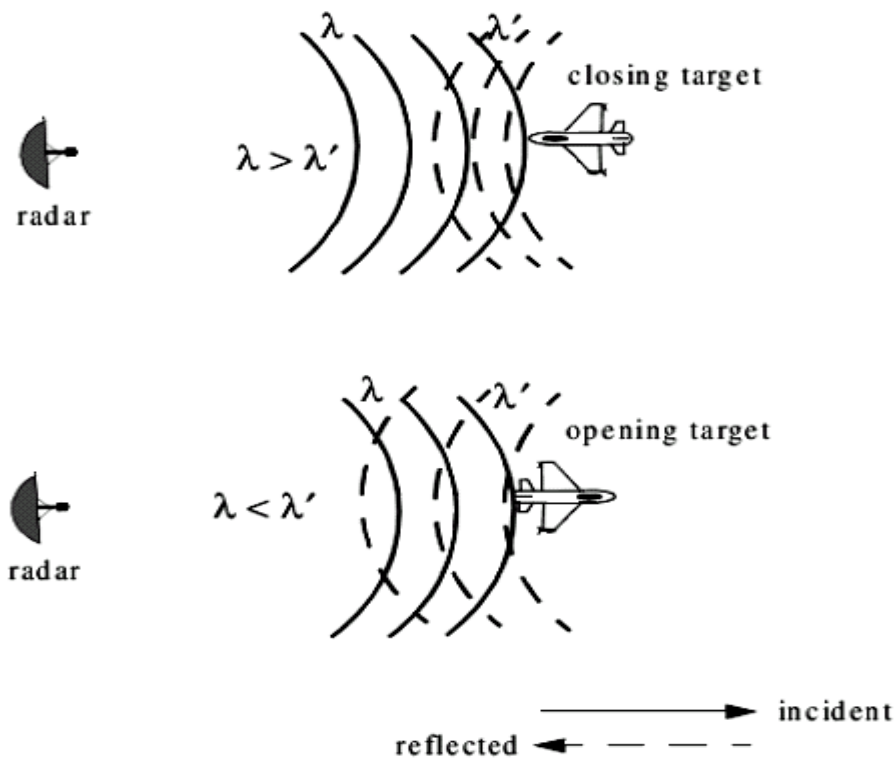


Figure 1.5. Effect of target motion on the reflected equiphase waveforms.

For a Doppler radar system to measure speed, an accurate sample of the original phase of the transmitted signal must be maintained for comparison against the reflected signal.

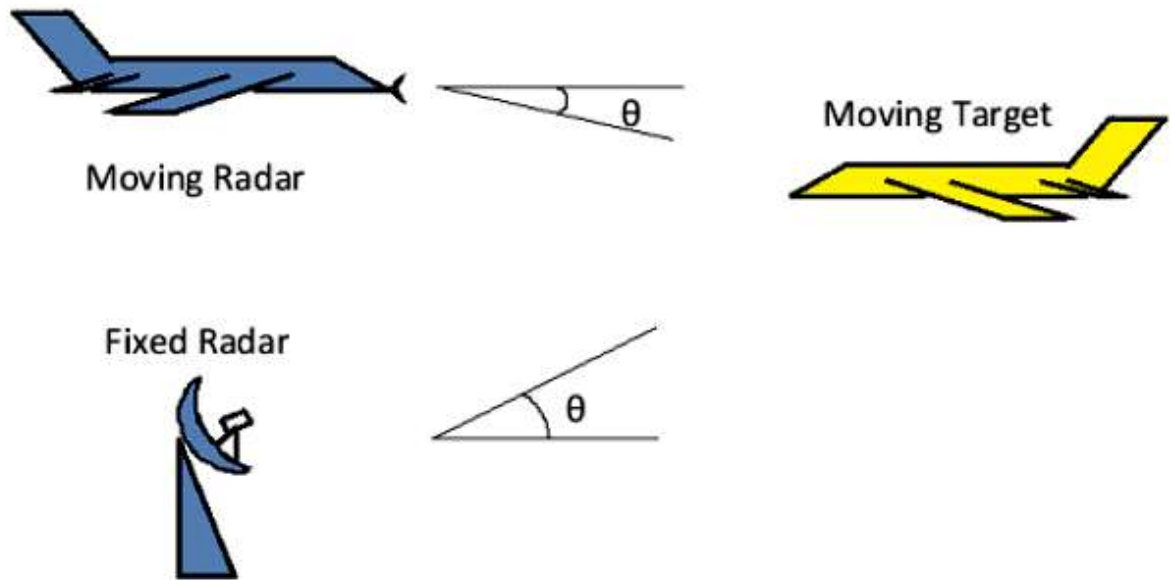


Figure 1.6. Doppler shift due to moving radar and targets

Angle shown (θ) is for elevation differences only; if there is also an azimuthal angle, it must be factored into the equation as $\cos(\alpha)$, where α is the azimuth angle relative to the radar antenna bore sight direction. For fixed radar with moving target:

$$f_D = 2V_T \cos\theta \frac{f_T}{c} \quad (1.8a)$$

For moving radar with moving target:

$$f_D = 2(V_R + V_T) \cos\theta \frac{f_T}{c} \quad (1.8b)$$

Where f_D = doppler frequency, f_T = transmitted frequency, V_T = target velocity, V_R = radar velocity, c = speed of light.

1.3.5. Coherence

A Radar is coherent if there is continuity in phase from one transmitted pulse to another. It is radar's ability to maintain an integer multiple of wavelengths between the equiphase wave fronts of any two successive pulses. Coherence is a requirement to measure (extract) the received signal phase. Since Doppler represents a frequency shift in the received signal, then only coherent or coherent-on-receive radars can extract Doppler information. This is because the instantaneous frequency of a signal is proportional to the time derivative of the signal phase. More precisely if f_i is the instantaneous frequency and $\varphi(t)$ is the signal phase.

$$f_i = \frac{1}{2\pi} \frac{d\varphi(t)}{dt} \quad (1.9)$$

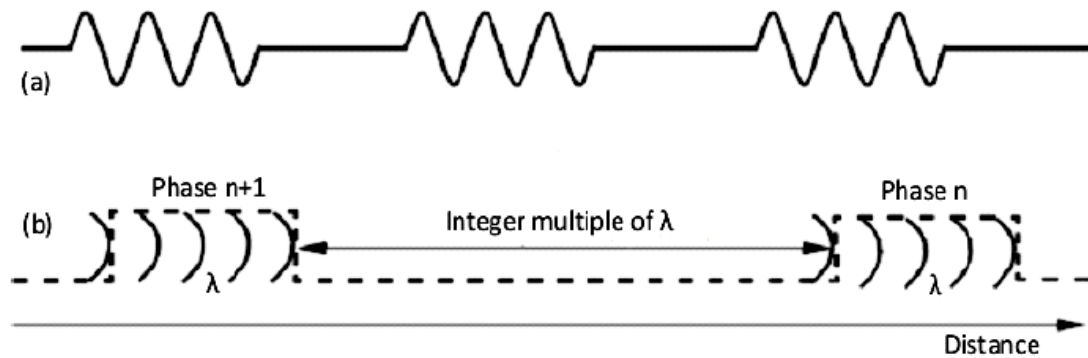


Figure 1.7. (a) Phase continuity between consecutive pulses.

(b) Maintaining an integer multiple of wavelengths between the equiphase wave fronts of any two successive pulses guarantees coherence.

1.4. Objective of the Thesis

The main objective of this thesis is to analyze the performance of pulse compression technique with different methods. The main purposes of the thesis are:

- To develop the mathematical model for basic radar system using relevant parameters.

- To study on side lobe reduction using pulse compression
- Increasing the resolution of a RADAR by this method.
- Achieving the energy of long pulse using short pulse.
- To study on decreasing average transmitted power
- To study on Analog & Digital pulse compression technique.
- Analysis the effects of noise, sampling rate and signal sparsity for pulse compression both in analog and digital system.
- To evaluate optimum result of various technique & compare among them.

1.5. Organization of the Thesis

Chapter 1 is an introductory chapter. It contains the origin and fundamentals of radar system.

Chapter 2 depicts the basic radar equations for both mono and bistatic radar.

Chapter 3 presents pulse compression fundamentals with necessary analysis. Different kind of weighting functions is also discussed here.

Chapter 4 deals with different kind of pulse compression techniques with necessary block diagram, simulations and mathematical models.

Chapter 5 analyzes the roles of weighting functions on matched filters. A cooperative study between different pulse compression techniques is shown here with necessary simulations. The improvement of range resolution performance for multiple targets by using Frank Code of length thirteen is identified.

Chapter 6 contains the concluding remarks and the scope of future works as well

Chapter 2

RADAR EQUATIONS AND PARAMETERS

2.1. Basic Radar Equation

2.1.1. Mono-static Radar Equation

The basic radar equation has many forms varying according to the parameters being used. The equation parameters vary according to the type and configuration of the radar in use. However, the most common form of the basic radar used is the monostatic radar where the same antenna is used for both transmitting and receiving. The basic radar equation for such monostatic radar system is developed below. First we consider a noiseless case and then we add the effects of noise to the basic equation.

2.1.2. Noiseless Case

Peak power density (power per unit area), P_D at range R from an Omni-directional radar with peak transmission power (P_t) is given by

$$P_D = \frac{P_t}{4\pi R^2} \quad (2.1)$$

When using directional antenna with gain G, the power density at a distance R is given by

$$P_D = \frac{P_t G}{4\pi R^2} \quad (2.2)$$

Here, gain depends on the effective aperture A_e of the antenna. Relation between gain and effective aperture area is

$$A_e = \frac{G\lambda^2}{4\pi} \quad (2.3)$$

The reflected power back to the target depends upon the target cross section σ . σ is also

called the radar cross section (RCS). σ is the ratio of the power reflected back to the radar (P_r) to the power density incident on the target (PD),

$$\frac{\sigma}{4\pi R^2} = \frac{P_r}{P_D} \quad (2.4)$$

Using Eq. 2.2 and Eq. 2.4, we can find the power delivered to the radar signal processor by the antenna (P_{D_r})

$$P_{D_r} = P_r A_e = P_D \frac{\sigma}{4\pi R^2} A_e = \frac{P_t G \sigma A_e}{(4\pi R^2)^2} \quad (2.5)$$

Substituting the value of A_e from Eq. 2.3 we get

$$P_{D_r} = \frac{P_t G^2 \lambda^2 \sigma}{(4\pi)^3 R^4} \quad (2.6)$$

Power delivered is the minimum when target is at maximum range (R_{max}). If we denote the minimum detectable power by S_{min} then from Eq. 2.6

$$R_{max} = \left(\frac{P_t G^2 \lambda^2 \sigma}{(4\pi)^3 S_{min}} \right)^{\frac{1}{4}} \quad (2.7)$$

This is the maximum range that can be achieved if we consider a noiseless medium and a lossless receiver.

2.1.3. With the Presence of Noise

In practical situations the returned signal is corrupted by noise which is a function of radar operating bandwidth, B . The input noise power to a lossless antenna is

$$N_i = k T_e B \quad (2.8)$$

Where, T_e is the total effective system noise temperature in Kelvin. The fidelity of a receiver is its ability to accurately reproduce, in its output, the signal that appears at its

input. The broader the band passed by frequency selection circuits, the greater is the receiver fidelity. The fidelity of a radar receiver is normally described by a figure of merit called the noise figure F .

$$F = \frac{(SNR)_i}{(SNR)_o} = \frac{\frac{S_i}{N_i}}{\frac{S_o}{N_o}} \quad (2.9)$$

Here $(SNR)_i$ and $(SNR)_o$ are SNR at input and output of receiver. S_i and N_i are input signal and noise power whereas S_o and N_o are output signal and noise power.

$$S_i = N_i(SNR)_o = kT_eBF(SNR)_o \quad (2.10)$$

Hence, the minimum detectable signal power can be written as

$$S_{min} = kT_eBF(SNR)_{o_{min}} \quad (2.11)$$

The radar detection threshold is set equal to this minimum output SNR, $(SNR)_{o_{min}}$. Substituting Eq. 2.11 in Eq. 2.7 and considering radar losses as L .

$$R_{max} = \left(\frac{P_t G^2 \lambda^2 \sigma}{(4\pi)^3 kT_e BFL(SNR)_{o_{min}}} \right)^{\frac{1}{4}} \quad (2.12)$$

Radar losses denoted as reduce the overall SNR, and hence

$$(SNR)_o = \frac{P_t G^2 \lambda^2 \sigma}{(4\pi)^3 kT_e BFLR^4} \quad (2.13)$$

Eq. 2.13 represents the basic equation for mono-static radar system.

2.2. Variations of Basic Equation

2.2.1. Bistatic Radar Equation

Bistatic radars use transmit and receive antennas that are placed in different locations. A synchronization link between the transmitter and receiver is necessary to provide the following information.

- The transmitted frequency in order to compute the Doppler shift.
- The transmit time or phase reference in order to measure the total scattered path.

Frequency and phase reference synchronization can be maintained through line-of-sight communications between the transmitter and receiver. However, if this is not possible, the receiver may use a stable reference oscillator for synchronization.

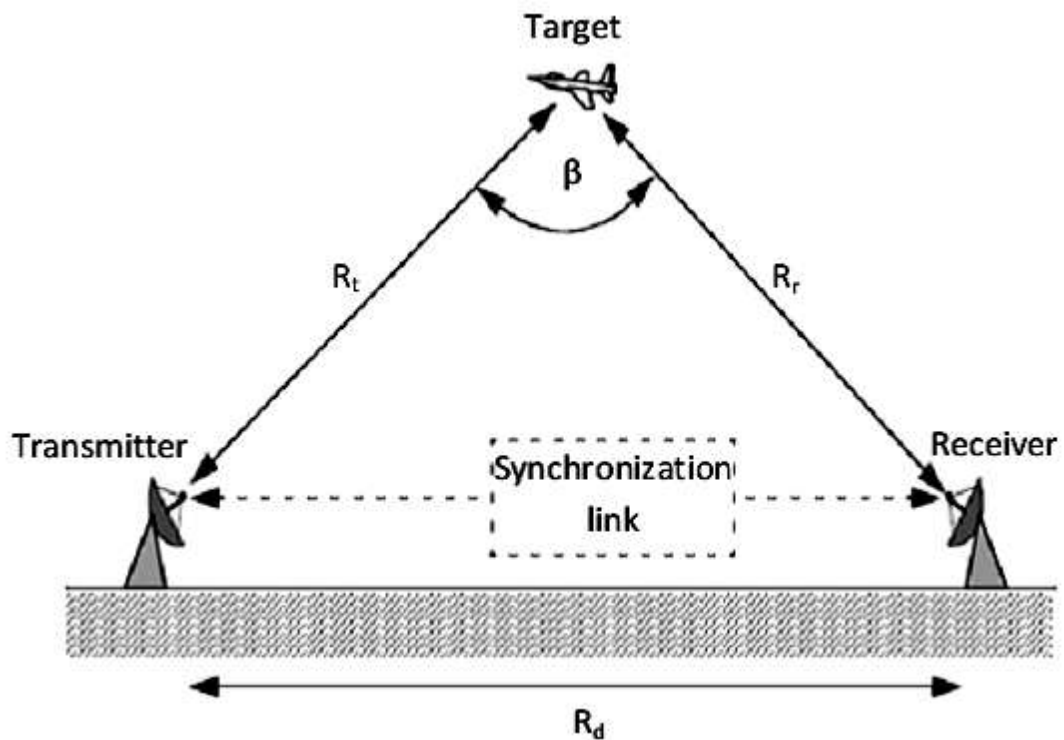


Figure 2.1. Bistatic radar geometry.

Fig. 2.1 shows the bistatic radar configuration. The angle β is called the bistatic angle. When β approaches 180° , the bistatic RCS becomes very large compared to the mono

static RCS which causes a change in the basic radar equation as given below

$$P_{D_r} = \frac{P_t G_t G_r \lambda^2 \sigma_B}{(4\pi)^3 R_t^2 R_r^2 L_t L_r L_p} \quad (2.14)$$

Here, P_{D_r} = total power delivered to the signal processor by the receiving antenna, P_t = peak transmitted power, G_t = Gain of transmitting antenna, G_r = Gain of receiving antenna, R_t = range from transmitter, R_r = range from receiver, L_t = transmitter losses, L_r = receiver losses, L_p = medium propagation loss. Here, a noiseless condition is assumed.

2.2.2. Low PRF Radar Equation

Consider a pulsed radar with pulse width τ , PRI T , and peak transmitted power P_t . The average transmitted power is $P_{av} = P_t d_t$, where d_t the transmission duty factor is $d_t = \tau/T$. We can define the receiving duty factor as

$$d_r = \frac{T - \tau}{T} = 1 - \tau f_r = 1 - \frac{\tau}{T} \quad (2.15)$$

Hence, for low PRF where, $T \gg \tau$, the receiving duty factor $d_r = 1$. Hence ignoring the impact of receiving duty factor low PRF radar equation for n_p coherent pulses ($n_p = T_i f_r$) can be written as following:

$$(SNR)_{n_p} = \frac{P_t G^2 \lambda^2 \sigma T_i f_r}{(4\pi)^3 R^4 k T_e B F L} = \frac{P_t G^2 \lambda^2 \sigma T_i f_r \tau}{(4\pi)^3 R^4 k T_e F L} \quad (2.16)$$

Here T_i = Time on target (time that a target is illuminated by the beam) and bandwidth $B = 1/\tau$. Since transmission duty factor is negligible compared to the receiving duty factor low PRF radars result in maximum unambiguous range thereby increasing overall range of the radar. We already defined time on target $T_i = n_p / f_r$; therefore, as the PRF, f_r is decreased time of the scanning beam on target is increased resulting in better output SNR. As a result low PRF radars give better SNR for targets at longer ranges.

2.2.3. High PRF Radar Equation

The central power spectrum line (DC component) for high PRF pulse train contains most of the signal's power. Its value is $(\tau/T)^2$, and it is equal to the square of the transmit duty factor. Thus, using Eq. 2.13, the single pulse radar equation for high PRF radar is

$$(SNR)_o = \frac{P_t G^2 \lambda^2 \sigma d_t^2}{(4\pi)^3 k T_e B F L R^4 d_r} \quad (2.17)$$

For high PRF radar, we cannot ignore d_r since $d_r = d_t = \tau f_r$. Again, for high PRF radar, $B = T_i$. Additionally, if we replace $P_{ave} = P_t \tau f_r$, then Eq. 2.17 becomes

$$SNR = \frac{P_{ave} T_i G^2 \lambda^2 \sigma}{(4\pi)^3 k T_e F L R^4} \quad (2.18)$$

Since $P_{ave} T_i$ in Eq. 2.17 is a kind of energy product therefore it indicates that high PRF radars can enhance detection performance by using relatively low power and longer integration time. Low PRF radars are used primarily for ranging where target velocity is not needed. High PRF radars are used for measuring target velocity (Doppler Shift).

Chapter 3

PULSE COMPRESSION FUNDAMENTALS

3.1. Matched Filter

The matched filter is the optimal linear filter for maximizing the signal to noise ratio (SNR) in the presence of additive stochastic noise. Matched filters are commonly used in radar, in which a signal is sent out, and we measure the reflected signals, looking for something similar to what was sent out. Two-dimensional matched filters are commonly used in image processing, e.g., to improve SNR for X-ray pictures.

The most unique characteristic of the matched filter is that it produces the maximum achievable instantaneous SNR at its output when a signal plus additive white noise are present at the input. The noise does not need to be Gaussian. The peak instantaneous SNR at the receiver output can be achieved by matching the radar receiver transfer function to the received signal. When the peak instantaneous signal power divided by the average noise power at the output of a matched filter is equal to twice the input signal energy divided by the input noise power, regardless of the waveform used by the radar. This is the reason why matched filters are often referred to as optimum filters in the SNR sense. Here the peak power used in the derivation of the radar equation (SNR) represents the average signal power over the duration of the pulse, not the peak instantaneous signal power as in the case of a matched filter. In practice, it is sometimes difficult to achieve perfect matched filtering. In such cases, sub-optimum filters may be used. Due to this mismatch, degradation in the output SNR occurs. Considering a radar system that uses finite duration energy signal $s_i(t)$, the pulse width as τ' and a matched filter receiver is utilized. The matched filter input signal can then be represented by

$$x(t) = C + s_i(t - t_1) + n_i(t) \quad (3.1)$$

Where C is a constant, t_1 is an unknown time delay proportional to the target range, and $n_i(t)$ is input white noise.

Since the input noise is white, its corresponding autocorrelation and Power Spectral Density (PSD) functions are given, respectively, by

$$\bar{R}_{n_i}(t) = \frac{N_0}{2} \delta(t) \quad (3.2)$$

$$\bar{S}_{n_i}(\omega) = \frac{N_0}{2} \quad (3.3)$$

where N_0 is a constant. $s_0(t)$ and $n_0(t)$ are denoted as the signal and noise filter outputs. More precisely, we can define

$$y(t) = C s_0(t - t_1) + n_0(t) \quad (3.4)$$

Where,

$$S_0(t) = S_i(t) \bullet h(t) \quad (3.5)$$

$$n_0(t) = n_i(t) \bullet h(t) \quad (3.6)$$

The operator (\bullet) indicates convolution, and $h(t)$ is the filter impulse response (the filter is assumed to be linear time invariant).

3.1.1. Matched Filter Replica

The coded signal can be described either by the frequency response $H(\omega)$ or as an impulse response $h(t)$ of the coding filter. The received echo is fed into a matched filter whose frequency response is the complex conjugate $H^*(\omega)$ of the coding filter. The

output of the matched filter, $y(t)$ is the compressed pulse which is just the inverse Fourier transform of the product of the signal spectrum and the matched filter response.

$$y(t) = \frac{1}{2\pi} \int_{-\infty}^{\infty} |H(\omega)|^2 \exp(j\omega t) d\omega \quad (3.7)$$

A filter is also matched if the signal is the complex conjugate of the time inverse of the filter's impulse-response. This is often achieved by applying the time inverse of the received signal to the pulse-compression filter.

The output of this matched filter is given by the convolution of the signal $h(t)$ with the conjugate impulse response $h^*(-t)$ of the matched filter,

$$y(t) = \int_{-\infty}^{\infty} h(\tau) h^*(t - \tau) d\tau \quad (3.8)$$

In essence the matched filter results in a correlation of the received signal with a delayed version of the transmitted signal as shown below.

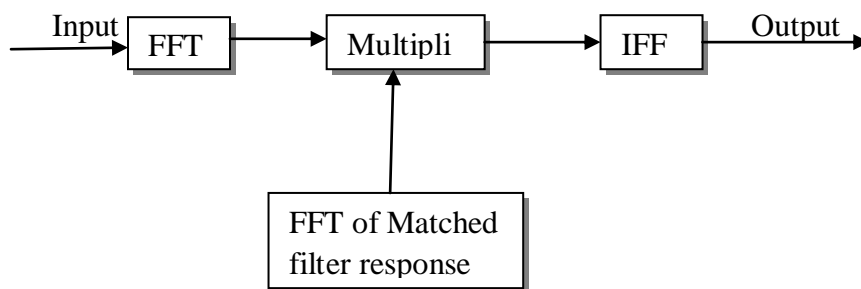


Figure 3.1. A block diagram of Pulse Compression based on FFT and Inverse FFT.

The range resolution of a sensor is defined as the minimum separation (in range) of two targets or equal cross section that can be resolved as separate targets. It is determined by the bandwidth of the transmitted signal. The range resolution is determined from the matched filter processing of the rectangular pulse. Considering the case that the transmitted signal consists of a constant frequency signal modulated by a rectangular

pulse of width, τ . The sharp edges of the rectangular function in time generate an infinite frequency spectrum.

In the continuous frequency (CF) example, the matched filter (correlation) response shows the triangular envelope. However, in the chirp example with the same duration, the matched filter generates a *sinc* function with a much narrower peak, and hence a superior range resolution. Also, the range resolution is inversely proportional to the chirp bandwidth, Δf .

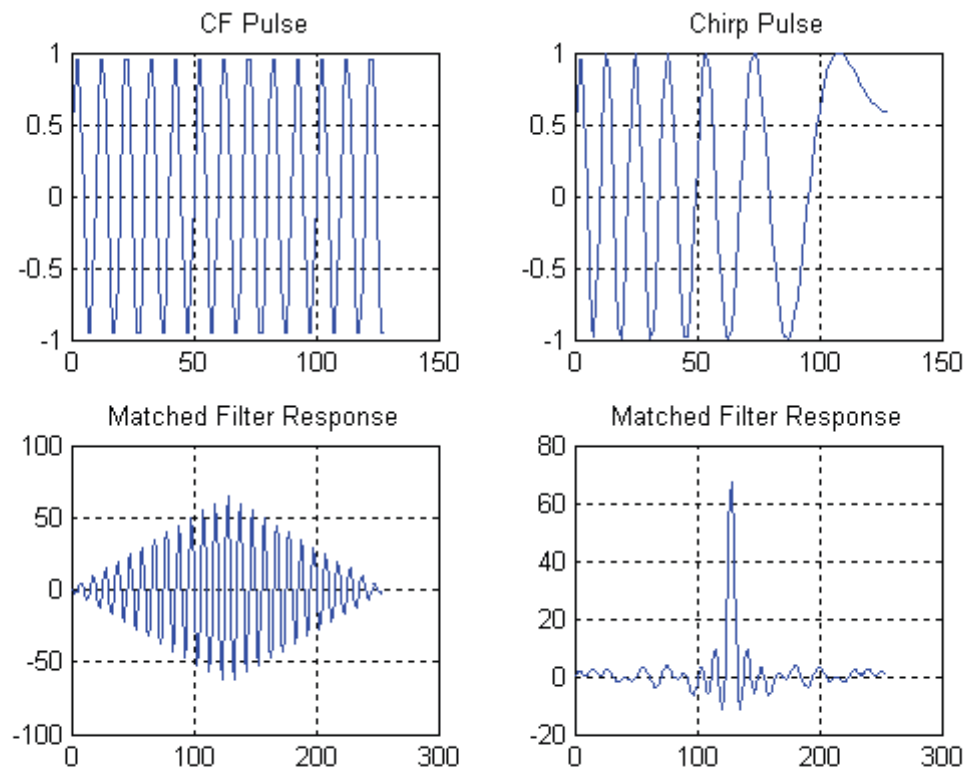


Figure 3.2. Comparison between the ultimate resolution of a rectangular constant frequency pulse and a chirp pulse of the same duration

3.2. The Radar Ambiguity Function

The radar ambiguity function represents the output of the matched filter, and it describes the interference caused by range and/or Doppler of a target when compared to a

reference target of equal RCS. The ambiguity function evaluated at (τ, f_d) is equal to the matched filter output that is matched perfectly to the signal reflected from the target of interest. In other words, returns from the nominal target are located at the origin of the ambiguity function. Thus, the ambiguity function at nonzero τ and f_d represents returns from some range and Doppler different from those for the nominal target.

The radar ambiguity function is normally used by radar designers as a means of studying different waveforms. It can provide insight about how different radar waveforms may be suitable for the various radar applications. It is also used to determine the range and Doppler resolutions for a specific radar waveform. The three-dimensional (3-D) plot of the ambiguity function versus frequency and time delay is called the radar ambiguity diagram. The radar ambiguity function for the signal $s(t)$ is defined as the modulus squared of its 2-D correlation function, i.e., $|\chi(\tau; f_d)|^2$. More precisely,

$$|\chi(\tau; f_d)|^2 = \left| \int_{-\infty}^{\infty} s(t) s^*(t + \tau) e^{j2\pi f_d t} dt \right|^2 \quad (3.9)$$

In this notation, the target of interest is located at $(\tau, f_d) = (0, 0)$ and the ambiguity diagram is centered at the same point. Note that some define the ambiguity function as $|\chi(\tau; f_d)|$. Here $|\chi(\tau; f_d)|$ is called the uncertainty function. We denote E as the energy of the signal $s(t)$,

$$E = \int_{-\infty}^{\infty} |s(t)|^2 dt \quad (3.10)$$

3.2.1. Properties of Radar Ambiguity Function

- The maximum value for the ambiguity function occurs at $(\tau, f_d) = (0, 0)$ and is equal to $4E^2$.

$$\max\{|\chi(\tau; f_d)|^2\} = |\chi(0; 0)|^2 = (2E)^2 \quad (3.11)$$

$$|\chi(\tau; f_d)|^2 \leq |\chi(0; 0)|^2 \quad (3.12)$$

- The ambiguity function is symmetric,

$$|\chi(\tau; f_d)|^2 = |\chi(-\tau; -f_d)|^2 \quad (3.13)$$

- The total volume under the ambiguity function is constant,

$$\iint |\chi(\tau; f_d)|^2 d\tau df_d = (2E)^2 \quad (3.14)$$

- If the function $S(f)$ is the Fourier transform of the signal $s(t)$, then by using Parseval's theorem we get,

$$|\chi(\tau; f_d)|^2 = \left| \int S^*(f) S(f - f_d) e^{-j2\pi f\tau} df \right|^2 \quad (3.15)$$

3.3. Correlation

Correlation is a mathematical relationship between two random variables or signals. In Statistics, correlation can be thought of as a normalized covariance. Correlation can be linear or circular. Generally speaking, linear correlation should be used when the input signals contain impulses, while circular correlation should be used when the signals repeat periodically.

Strength of correlation is expressed by a correlation coefficient. Let $f(n)$ and $g(n)$ be two signals of the same length, M . Their correlation coefficient can be defined as:

$$y(m) = \sum_{n=0}^{M-1} f(n)g(n - m) \quad (3.16)$$

If the input signals are not of the same length, the shorter one will be zero-padded to the length of the other signal. For linear correlation, the length of the result sequence is $2M - 1$, while the length of the result sequence for circular correlation is M . The magnitude of the computed correlation coefficient shows the degree of similarity between the signals. If the magnitude is large, the two signals have a strong linear relationship. Alternatively, if the magnitude is small, the two signals can be considered to have little or no linear relationship.

If the correlation coefficient is normalized (the Normalize checkbox is selected), its absolute value will range from 0 to 1, making it easier to judge the similarity between the signals. If the normalized correlation coefficient is equal to either 1 or -1, the two signals are perfectly correlated. The sign of the correlation coefficient indicates the direction of association. A positive correlation suggests that the change of one signal will cause the other signal to change in the same direction; a positive linear relationship. If the correlation is negative, a negative linear relationship exists; an increase in one signal will cause a decrease in the other.

3.3.1. To Use Correlation

- Make a workbook or a graph active.
- Select Analysis: Signal Processing: Correlation from the Origin menu

3.3.2. Cross-correlation

In signal processing, cross-correlation is a measure of similarity of two waveforms as a function of a time-lag applied to one of them. This is also known as a sliding dot product or sliding inner-product. It is commonly used for searching a long signal for a shorter, known feature. It has applications in pattern recognition, single particle analysis, electron tomographic averaging, cryptanalysis, and neurophysiology. For continuous functions f and g , the cross-correlation is defined as:

$$(f * g)(t) \stackrel{\text{def}}{=} \int_{-\infty}^{\infty} f^*(\tau) g(t + \tau) d\tau \quad (3.17)$$

where f^* denotes the complex conjugate of f .

Similarly, for discrete functions, the cross-correlation is defined as:

$$(f * g)[n] \stackrel{\text{def}}{=} \sum_{m=-\infty}^{\infty} f^*[m] g[n + m] \quad (3.18)$$

The cross-correlation is similar in nature to the convolution of two functions.

3.3.2.1. Properties

- The cross-correlation of functions $f(t)$ and $g(t)$ is equivalent to the convolution of $f^*(-t)$ and $g(t)$.

$$f * g = f^*(-t) * g \quad (3.19)$$

- If f is Hermitian, then $f * g = f * g$
 - $(f * g) * (f * g) = (f * f) * (g * g)$
- (3.20)

- Analogous to the convolution Theorem, the cross-correlation satisfies:

$$F\{f * g\} = (F\{f\})^* \cdot F\{g\} \quad (3.21)$$

where F denotes the Fourier Transform, and an asterisk again indicates the complex conjugate. Coupled with Fast Fourier Transform algorithms, this property is often exploited for the efficient numerical computation of cross-correlations.

- The cross-correlation is related to the spectral density.

- The cross correlation of a convolution of f and h with a function g is the convolution of the cross-correlation of f and g with the kernel h :

$$(f * h) * g = h(-) * (f * g) \quad (3.22)$$

3.3.3. Auto-correlation

Autocorrelation is the cross-correlation of a signal with itself. Informally, it is the similarity between observations as a function of the time lag between them. It is a mathematical tool for finding repeating patterns, such as the presence of a periodic signal obscured by noise, or identifying the missing fundamental frequency in a signal implied by its harmonic frequencies. It is often used in signal processing for analyzing functions or series of values, such as time domain signals. In signal processing, the above definition is often used without the normalization, that is, without subtracting the mean and dividing by the variance. When the autocorrelation function is normalized by mean and variance, it is sometimes referred to as the autocorrelation coefficient.

Given a signal $f(t)$, the continuous autocorrelation $R_{ff}(\tau)$ is most often defined as the continuous cross-correlation integral of $f(t)$ with itself, at lag τ .

$$R_{ff}(\tau) = (f(t) * \bar{f}(-t))(\tau) = \int_{-\infty}^{\infty} f(t) \bar{f}(t - \tau) dt \quad (3.23)$$

where \bar{f} represents the complex conjugate and $*$ represents convolution. For a real function, $\bar{f} = f$.

The discrete autocorrelation R at lag j for a discrete signal x_n is

$$R_{xx}(j) = \sum_n x_n \bar{x}_{n-j} \quad (3.24)$$

3.3.3.1. Properties

In the following, we will describe properties of one-dimensional autocorrelations only, since most properties are easily transferred from the one-dimensional case to the multi-dimensional cases.

- A fundamental property of the autocorrelation is symmetry, $R(i) = R(-i)$, which is easy to prove from the definition. In the continuous case, the autocorrelation is an even function $R_f(-\tau) = R_f(\tau)$ when f is a real function, and the autocorrelation is a Hermitian function $R_f(-\tau) = R_f^*(\tau)$ when f is a complex function.
- The continuous autocorrelation function reaches its peak at the origin, where it takes a real value, i.e. for any delay τ , $|R_f(\tau)| \leq R_f(0)$. This is a consequence of the Rearrangement inequality. The same result holds in the discrete case.
- The autocorrelation of a periodic function is, itself, periodic with the same period.
- The autocorrelation of the sum of two completely uncorrelated functions (the cross-correlation is zero for all τ) is the sum of the autocorrelations of each function separately.
- Since autocorrelation is a specific type of cross-correlation, it maintains all the properties of cross-correlation.
- The autocorrelation of a continuous-time white-noise signal will have a strong peak (represented by a Dirac Delta Function) at $\tau = 0$ and will be absolutely 0 for all other τ .

The transmitted sequence is loaded into the reference register, and the input sequence is continuously clocked through the signal shift register. A comparison counter forms a sum of the matches and subtracts the mismatches between

corresponding stages of the shift registers on every clock cycle to produce the correlation function.

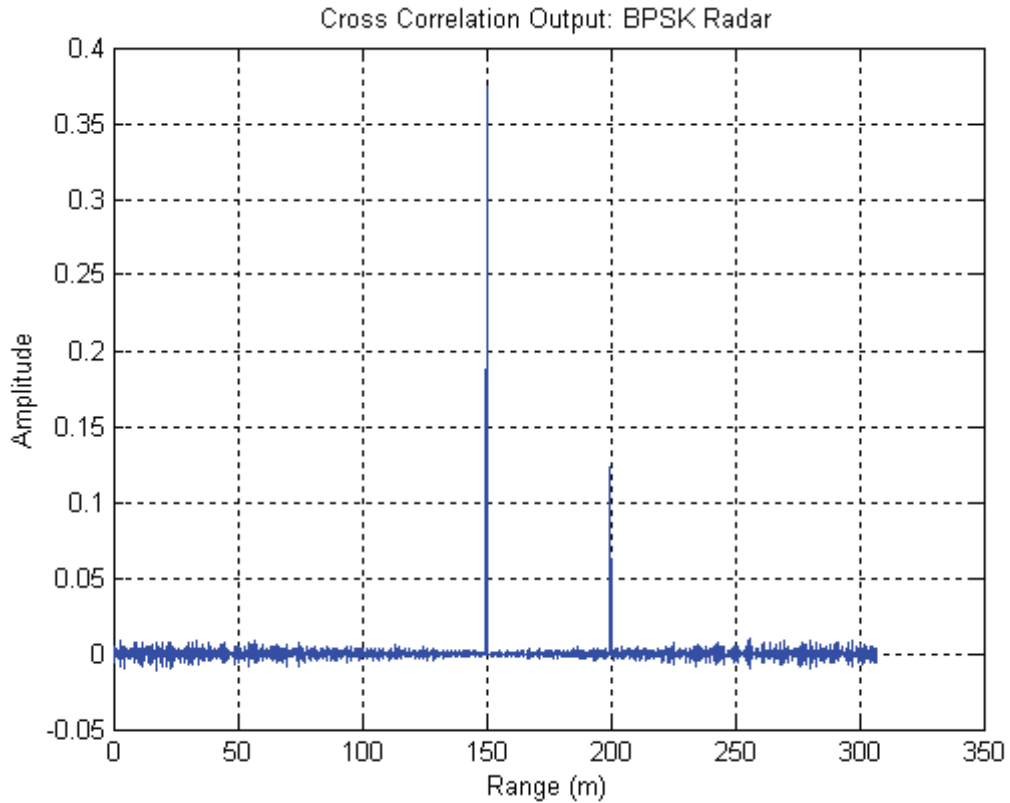


Figure 3.3. Cross correlation showing two targets with different amplitudes and at different ranges: BPSK radar noise sequence generated using a 12bit shift register with 4096 points.

The Maximal Length series must be an odd number, and by padding with zeros degrades the range sidelobe performance. To test this, the correct (unpadded) series was generated and the correct correlation function performed on 4095 points with the following incredible results.

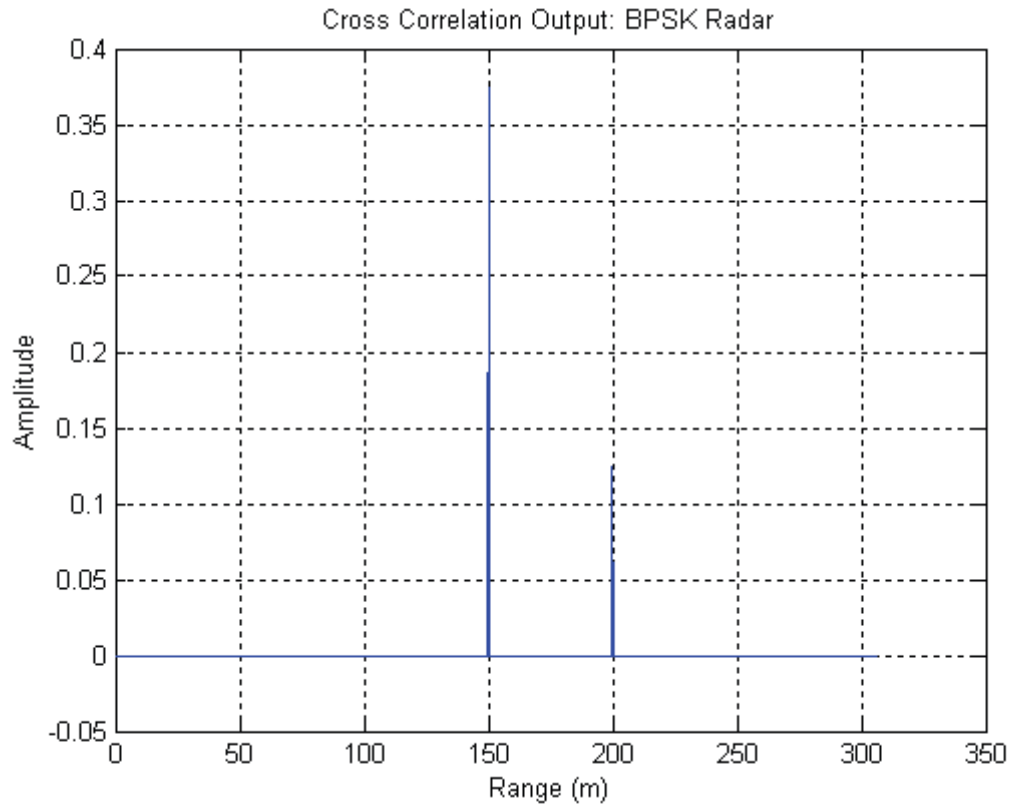


Figure 3.4. Cross correlation showing two targets with different amplitudes and at different ranges: BPSK radar noise sequence generated using a 12bit shift register with 4095 points

If the figure is examined carefully, it can be seen that the side lobe level is constantly flat with a value slightly smaller than zero (-1.22×10^{-4}).

3.4. Weighting Functions

In signal processing, a window function (also known as an apodization function or tapering function) is a mathematical function that is zero-valued outside of some chosen interval. When another function or waveform/data-sequence is multiplied by a window function, the product is also zero-valued outside the interval: all that is left is the part where they overlap; the "view through the window". Applications of window functions include spectral analysis, filter design, and beam forming. In typical applications, the

window functions used are non-negative smooth "bell-shaped" curves, though rectangle, triangle, and other functions can be used.

A more general definition of window functions does not require them to be identically zero outside an interval, as long as the product of the window multiplied by its argument is square integrable, that is, that the function goes sufficiently rapidly toward zero. Windowing of a simple waveform like $\cos \omega t$ causes its Fourier transform to develop non-zero values (commonly called spectral leakage) at frequencies other than ω . The leakage tends to be worst (highest) near ω and least at frequencies farthest from ω . If the waveform under analysis comprises two sinusoids of different frequencies, leakage can interfere with the ability to distinguish them spectrally. If their frequencies are dissimilar and one component is weaker, then leakage from the larger component can obscure the weaker one's presence. But if the frequencies are similar, leakage can render them irresolvable even when the sinusoids are of equal strength.

3.4.1. Rectangular Window

A function that is constant inside the interval and zero elsewhere is called a rectangular window, which describes the shape of its graphical representation. The rectangular window has excellent resolution characteristics for sinusoids of comparable strength, but it is a poor choice for sinusoids of disparate amplitudes. This characteristic is sometimes described as low-dynamic-range.

Definition (M odd):

$$w_R(n) \triangleq \begin{cases} 1, & |n| \leq (M-1)/2 \\ 0, & \text{otherwise} \end{cases} \quad (3.25)$$

Transform:

$$W_R(\omega) = M \cdot \text{sinc}_M(\omega) \triangleq \frac{\sin\left(\frac{M\omega}{2}\right)}{\sin\left(\frac{\omega}{2}\right)} \quad (3.26)$$

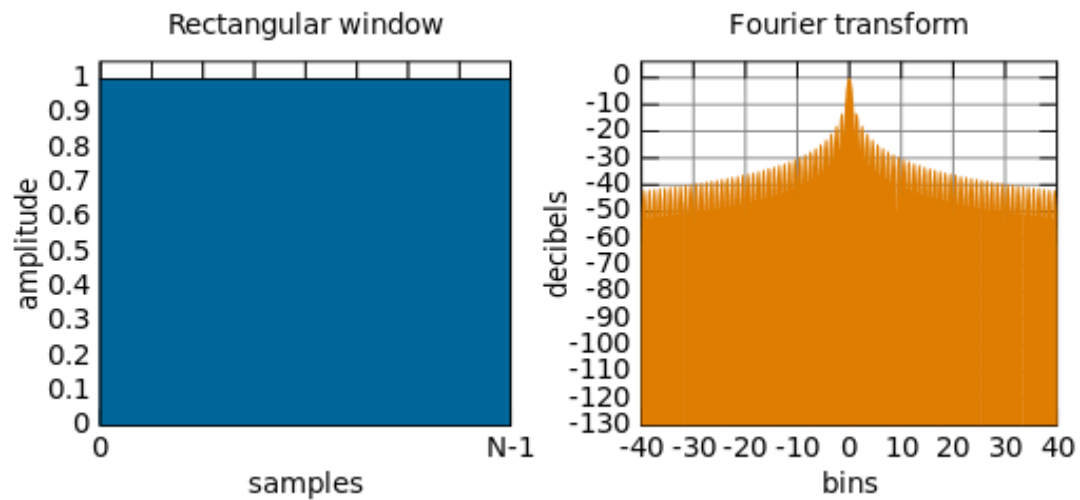


Figure 3.5. Rectangular Window

3.4.1.1. Properties

- Zero crossings at integer multiples of

$$\Omega_M \triangleq \frac{2\pi}{M} = \text{frequency sampling interval for a length } M \text{ DFT} \quad (3.27)$$

- Main lobe width is $2\Omega_M = \frac{4\pi}{M}$ (3.28)
- As M increases, the main lobe narrows (better frequency resolution).
- M has no effect on the height of the side lobes
- First side lobe only 13 dB down from the main-lobe peak.
- Side lobes roll off at approximately 6dB per octave.
- A phase term arises when we shift the window to make it causal, while the window transform is real in the zero-phase case (*i.e.*, centered about time 0)

3.4.2. Kaiser Window

The Kaiser window, also known as the Kaiser-Bessel window, was developed by James Kaiser at Bell Laboratories. It is a one-parameter family of window functions used for digital signal processing, and is defined by the formula,

$$w(n) = \frac{I_0[2\pi\sqrt{1 - (2n/N)^2}]}{I_0(2\pi)} \quad (3.29)$$

Where,

- N is the length of the sequence.
- I_0 is the zeroth order Modified Bessel function of the first kind.
- α is an arbitrary, non-negative real number that determines the shape of the window. In the frequency domain, it determines the trade-off between main-lobe width and side lobe level, which is a central decision in window design.

When N is an odd number, the peak value of the window is $w[(N - 1)/2] = 1$ and when N is even, the peak values are $w[(N/2) - 1] = w[\frac{N}{2}] < 1$

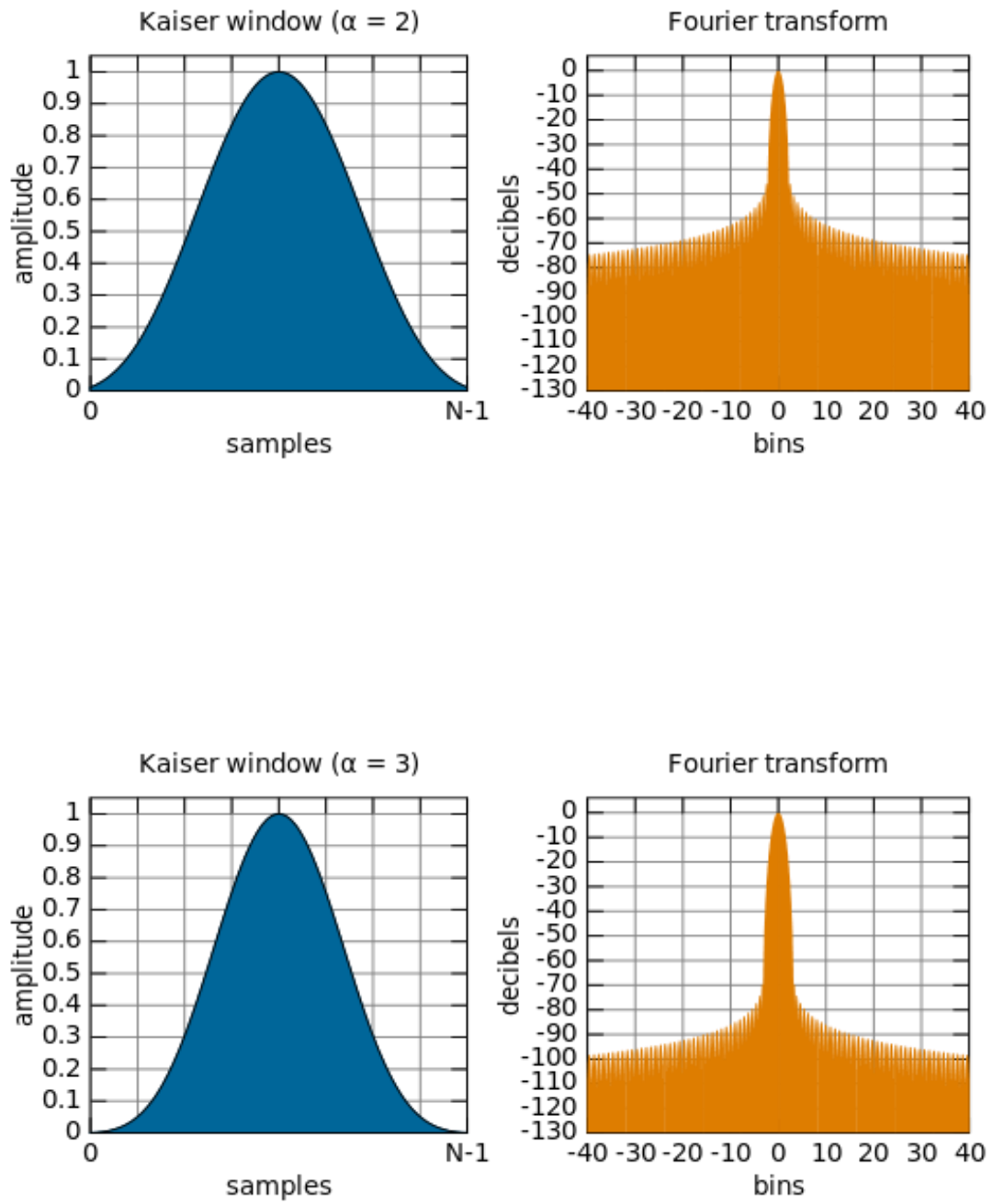


Figure 3.6. Kaiser Window

3.4.3. Hamming Window

The window with these particular coefficients was proposed by Richard W. Hamming. The window is optimized to minimize the maximum (nearest) side lobe, giving it a height of about one-fifth that of the Hanning window.

$$w(n) = \alpha - \beta \left[1 - \cos\left(\frac{2\pi n}{N-1}\right) \right] \quad (3.30)$$

Where $\alpha = 0.54$ and $\beta = 1 - \alpha = 0.46$

Instead of both constants being equal to 1/2 in the Hanning window. The constants are approximations of values $\alpha = 25/46$ and $\beta = 21/46$, which cancel the first side lobe of the Hanning window by placing a zero at frequency $5\pi/(N-1)$. Approximation of the constants to two decimal places substantially lowers the level of side lobes, to a nearly equiripple condition. In the equiripple sense, the optimal values for the coefficients are $\alpha = 0.53836$ and $\beta = 0.46164$.

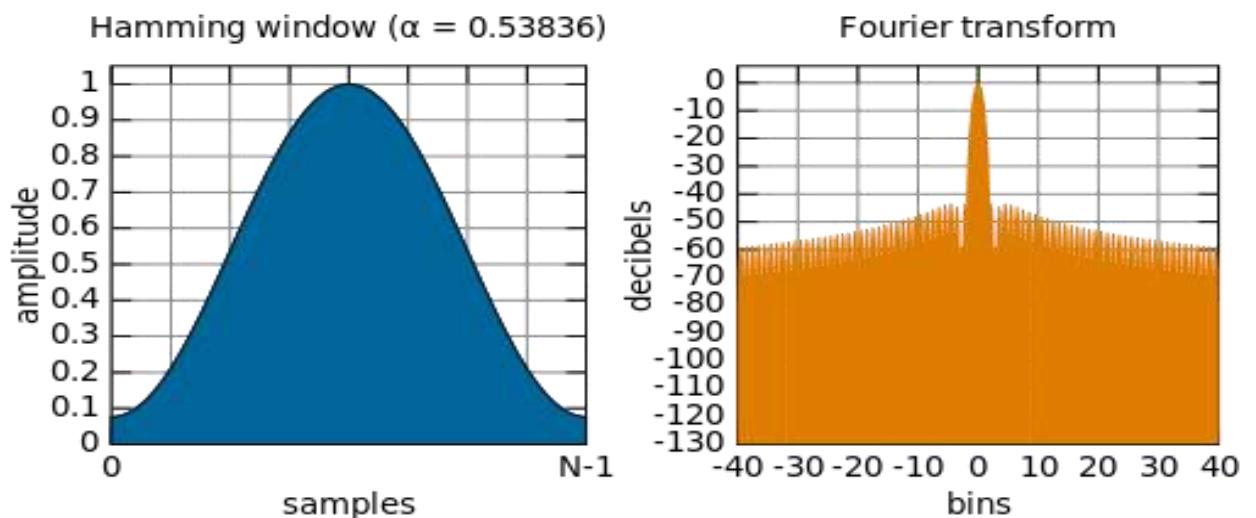


Figure 3.7. Hamming Window

3.4.4. Chebyshev Window

The Chebyshev window minimizes the mainlobe width, given a particular sidelobe height. It is characterized by an equiripple behavior, that is, its sidelobes all have the same height. The chebwin function, with length and sidelobe height parameters, computes a Chebyshev window.

$$w(n) = \frac{1}{N} \left[\frac{1}{r} + 2 \sum_{i=1}^{(N-1)/2} T_{N-1} \left(x_0 \cos \left(\frac{i\pi}{N} \right) \right) \cos \left(\frac{2\pi ni}{N} \right) \right] \quad (3.31)$$

Where I_0 is the zero-order modified Bessel function of the first kind and

$$x_0 = \cosh \left(\frac{1}{N-1} \cosh^{-1} \left(\frac{1}{r} \right) \right) \quad (3.32)$$

If A is the side lobe attenuation in dB. Then

$$\frac{1}{r} = 10^{-A/20} \quad (3.33)$$

And

$$T_N(x) = \begin{cases} \cos(n \cos^{-1}(x)) & |x| \leq 1 \\ \cosh(n \cosh^{-1}(x)) & |x| > 1 \end{cases} \quad (3.34)$$

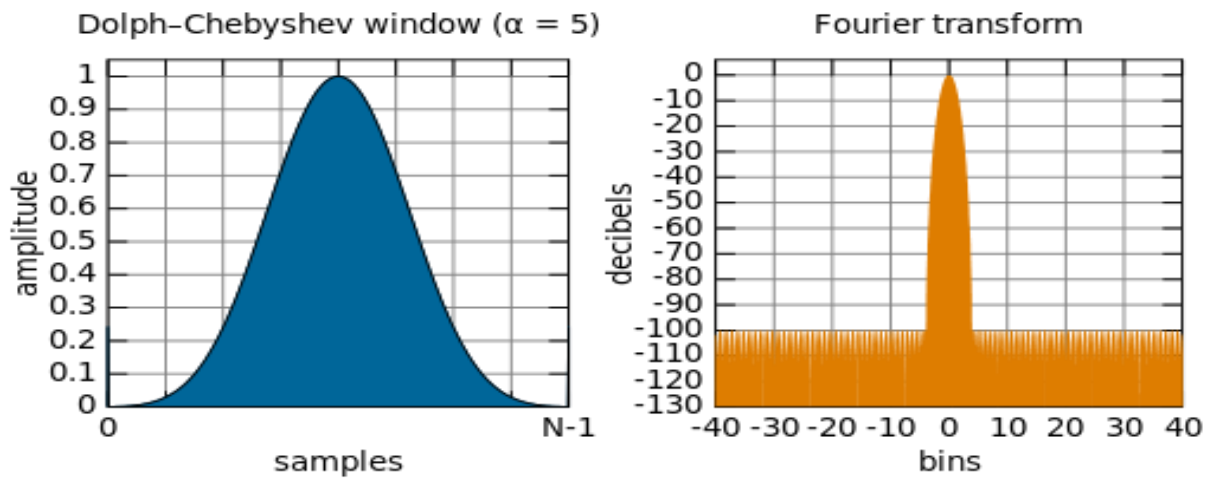


Figure 3.8. Chebyshev Window

Chapter 4

PULSE COMPRESSION

4.1. Definition

Pulse compression is a generic term that is used to describe a wave shaping process that is produced as a propagating waveform is modified by the electrical network properties of the transmission line. The pulse is frequency modulated, which provides a method to further resolve targets which may have overlapping returns. Pulse compression originated with the desire to amplify the transmitted impulse (peak) power by temporal compression. Range resolution for a given radar can be significantly improved by using very short pulses. Unfortunately, utilizing short pulses decreases the average transmitted power, which can hinder the radar's normal modes of operation, particularly for multi-function and surveillance radars. Since the average transmitted power is directly linked to the receiver SNR, it is often desirable to increase the pulse width (i.e., increase the average transmitted power) while simultaneously maintaining adequate range resolution. This can be made possible by using pulse compression techniques. The compression ratio is equal to the number of sub pulses in the waveform, i.e., the number of elements in the code. The range resolution is therefore proportional to the time duration of one element of the code. The radar maximum range is increased by the fourth root of PCR.

Pulse compression is a signal processing technique mainly used in radar, sonar and echography to increase the range resolution as well as the signal to noise ratio. This is achieved by modulating the transmitted pulse and then correlating the received signal with the transmitted pulse. Pulse compression allows us to achieve the average transmitted power of a relatively long pulse, while obtaining the range resolution corresponding to a short pulse. In this chapter, we will analyze analog and digital pulse compression techniques. Two analog pulse compression techniques are discussed in this chapter. The first technique is known as “correlation processing” which is dominantly

used for narrow band and some medium band radar operations. The second technique is called “stretch processing” and is normally used for extremely wide band radar operations. Digital pulse compression will also be briefly presented.

4.2. Time-Bandwidth Product

Consider a radar system that employs a matched filter receiver. Let the matched filter receiver bandwidth be denoted as B . Then, the noise power available within the matched filter bandwidth is given by

$$N_i = 2 \frac{N_o}{2} \quad (4.1)$$

Where the factor of two is used to account for both negative and positive frequency bands, as illustrated in Fig. 4.1

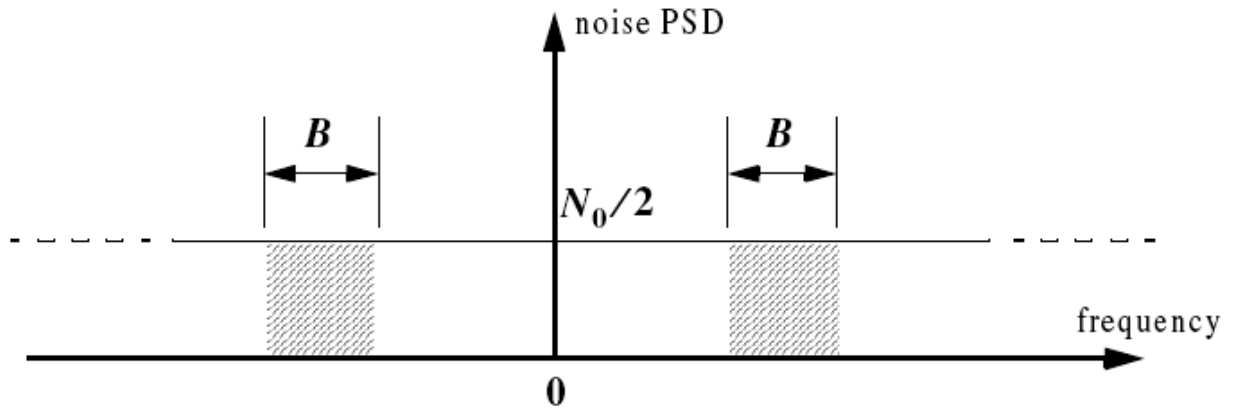


Figure 4.1. Input noise power

The average input signal power over a pulse duration τ' is

$$S_i = \frac{E}{\tau'} \quad (4.2)$$

E is the signal energy. Consequently, the matched filter input SNR is given by

$$(SNR)_i = \frac{S_i}{N_i} = \frac{E}{N_o B \tau'} \quad (4.3)$$

Again we know that

$$SNR(t_o) = \frac{2E}{N_o} \quad (4.4)$$

Now, combining equation 4.3 & 4.4 we may compute the output peak instantaneous SNR to the input SNR ratio as

$$\frac{SNR(t_o)}{(SNR)_i} = 2B\tau' \quad (4.5)$$

The quantity $B\tau'$ is referred to as the “time-bandwidth product” for a given waveform, or its corresponding matched filter. The factor $B\tau'$ by which the output SNR is increased over that at the input is called the matched filter gain, or simply the compression gain.

In general, the time-bandwidth product of an unmodulated pulse approaches unity. The time-bandwidth product of a pulse can be made much greater than unity by using frequency or phase modulation. If the radar receiver transfer function is perfectly matched to that of the input waveform, then the compression gain is equal to $B\tau'$. Clearly, the compression gain becomes smaller than $B\tau'$ as the spectrum of the matched filter deviates from that of the input signal.

4.3. Radar Equation with Pulse Compression

The radar equation for a pulsed radar can be written as

$$SNR = \frac{P_t \tau' G^2 \lambda^2 \sigma}{(4\pi)^3 R^4 k T_e F L} \quad (4.6)$$

Where P_t is the peak power, τ' is pulse width, G is the antenna gain, σ is the target RCS, R is range, k is Boltzman's constant, T_e is effective noise temperature, F is noise figure, and L is total radar losses.

Pulse compression radars transmit relatively long pulses (with modulation) and process the radar echo into very short pulses (compressed). One can view the transmitted pulse to be composed of a series of very short sub-pulses (duty is 100%), where the width of each sub-pulse is equal to the desired compressed pulse width. Denote the compressed pulse width as τ_c . Thus, for an individual sub-pulse, Eq. (4.6) can be written as

$$(SNR)_{\tau_c} = \frac{P_t \tau' G^2 \lambda^2 \epsilon}{(4\pi)^3 R^4 k T_e FL} \quad (4.7)$$

The SNR for the uncompressed pulse is then derived from Eq. (4.7) as

$$SNR = \frac{P_t (\tau' = n\tau_c) G^2 \lambda^2 \epsilon}{(4\pi)^3 R^4 k T_e FL} \quad (4.8)$$

Where n is the number of sub-pulses. Equation (4.8) is denoted as the radar equation with pulse compression.

Observation of Eq. (4.5) and (4.7) indicates the following (note that both equations have the same form): For a given set of radar parameters, and as long as the transmitted pulse remains unchanged, then the SNR is also unchanged regardless of the signal bandwidth. More precisely, when pulse compression is used, the detection range is maintained while the range resolution is drastically improved by keeping the pulse width unchanged and by increasing the bandwidth. Remember that range resolution is proportional to the inverse of the signal bandwidth,

$$\Delta R = C/2B \quad (4.9)$$

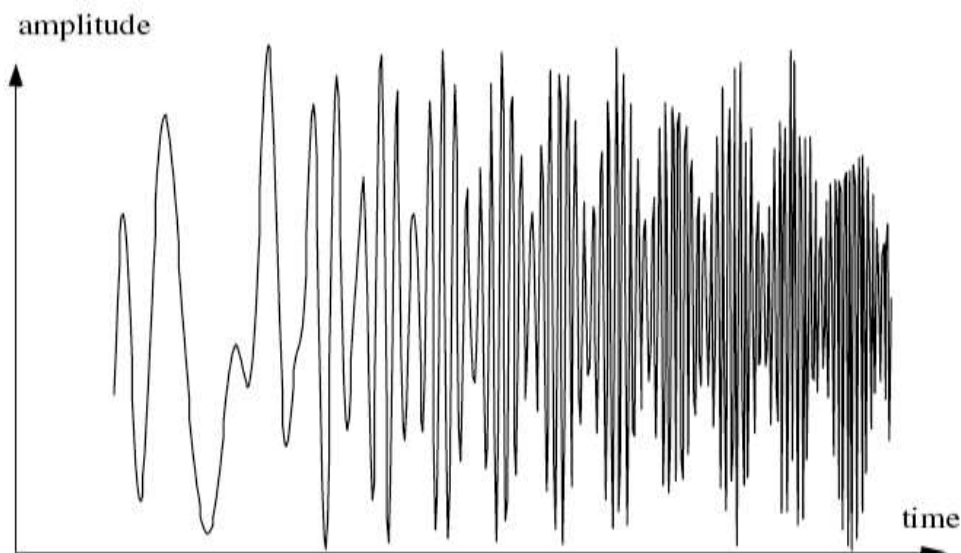
4.4. Analog Pulse Compression

Correlation and stretch pulse compression techniques are discussed in this section.

4.4.1. Correlation Processor

In this case, pulse compression is accomplished by adding frequency modulation to a long pulse at transmission, and by using a matched filter receiver in order to compress the received signal. Using LFM within a rectangular pulse compresses the matched filter output by a factor $\xi = B\tau'$, which is directly proportional to the pulse width and achieve large compression ratios. This form of pulse compression is known as “correlation processing.”

Fig. 4.2 illustrates the advantage of pulse compression. In this example, an LFM waveform is used. Two targets with RCS $\sigma_1 = 1m^2$ and $\sigma_2 = 0.5m^2$ are detected. The two targets are not separated enough in time to be resolved. Fig. 4.2a shows the composite echo signal from those targets. Clearly, the target returns overlap and, thus, they are not resolved. However, after pulse compression the two pulses are completely separated and are resolved as two targets. In fact, when using LFM, returns from neighboring targets are resolved as long as they are separated, in time, by τ_{n_1} , the compressed pulse width.



Figure

Figure 4.2. (a) Composite echo signal for two unresolved targets.

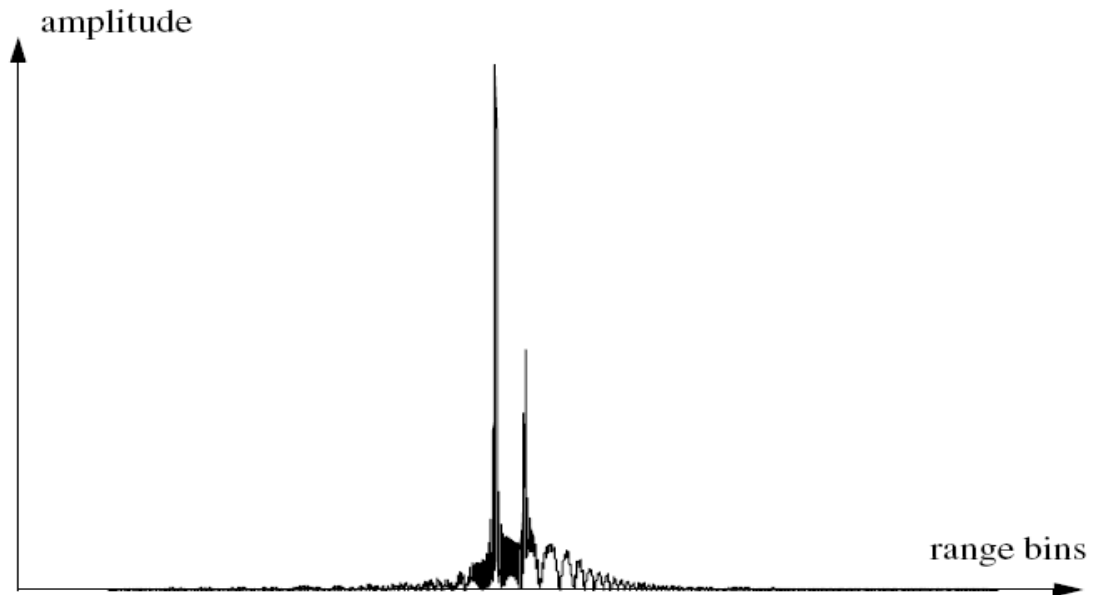


Figure 4.2. (b) Composite echo signal corresponding to Fig. 4.2a, after pulse compression.

Radar operations (search, track, etc.) are usually carried out over a specified range window, referred to as the receive window and defined by the difference between the radar maximum and minimum range. Returns from all targets within the receive window are collected and passed through a matched filter circuitry to perform pulse compression. One implementation of such analog processors is the Surface Acoustic Wave (SAW) devices. Because of the recent advances in digital computer development, the correlation processor is often performed digitally using the FFT. This digital implementation is called Fast Convolution Processing (FCP) and can be implemented at base-band. The fast convolution process is illustrated in Fig. 4.3

Since the matched filter is a linear time invariant system, its output can be described mathematically by the convolution between its input and its impulse response,

$$y(t) = s(t) \cdot h(t) \quad (4.10)$$

Where $s(t)$ is the input signal, $h(t)$ is the matched filter impulse response (replica), and the (\bullet) operator symbolically represents convolution. From the Fourier transform properties,

$$FFT\{s(t) \bullet h(t)\} = S(f) \cdot H(f) \quad (4.11)$$

And when both signals are sampled properly, the compressed signal can be computed from

$$y = FFT^{-1}\{S \cdot H\} \quad (4.12)$$

Where FFT^{-1} is the reverse of FFT . When using pulse compression, it is desirable to use modulation schemes that can accomplish a maximum pulse compression ratio, and can significantly reduce the side lobe levels of the compressed waveform. For the LFM case the first side lobe is approximately 13.4 dB below the main peak, and for most radar applications this may not be sufficient. In practice, high side lobe levels are not preferable because noise and/or jammers located at the side lobes may interfere with target returns in the main lobe.

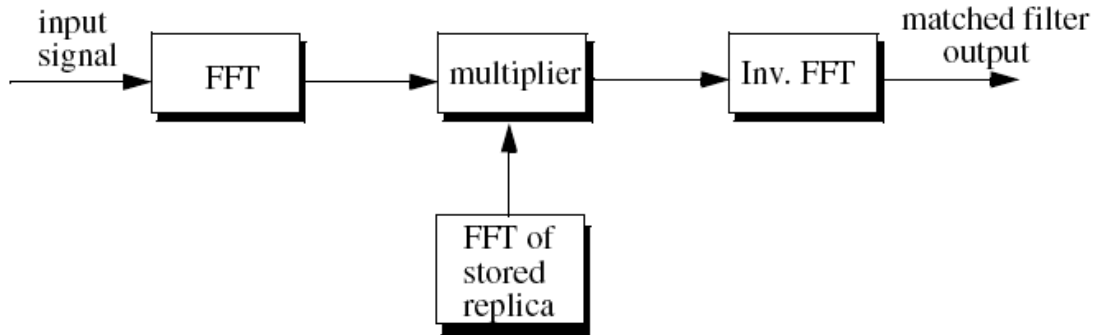


Figure 4.3. Computing the matched filter output using an FFT.

Weighting functions (windows) can be used on the compressed pulse spectrum in order to reduce the side lobe levels. The cost associated with such an approach is a loss in the main lobe resolution, and a reduction in the peak value (i.e., loss in the SNR), as

illustrated in Fig. 4.4. Weighting the time domain transmitted or received signal instead of the compressed pulse spectrum will theoretically achieve the same goal. However, this approach is rarely used, since amplitude modulating the transmitted waveform introduces extra burdens on the transmitter.

Consider a radar system that utilizes a correlation processor receiver (i.e., matched filter). The receive window in meters is defined by

$$R_{rec} = R_{max} - R_{min} \quad (4.13)$$

Where R_{max} and R_{min} respectively, define the maximum and minimum range over which the radar performs detection. Typically R_{rec} is limited to the extent of the target complex.

The radar echo signal is similar to the transmitted one with the exception of a time delay and an amplitude change that correspond to the target RCS. The first step of the processing consists of removing the frequency f_0 .

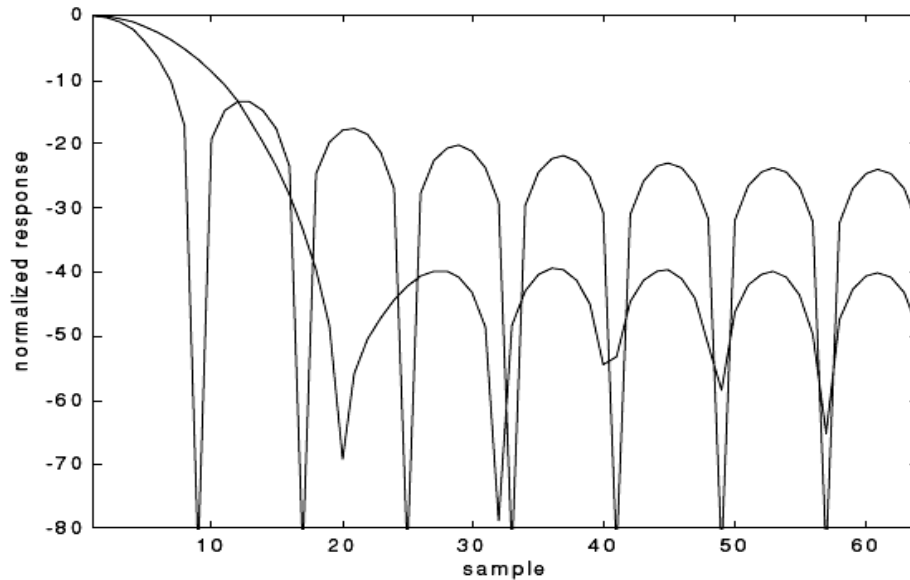


Figure 4.4. Reducing the first side lobe to -42 dB doubles the main lobe width.

By using MATLAB Function we can get the uncompressed and compressed echo signal in Fig. 4.5 and Fig. 4.6 respectively.

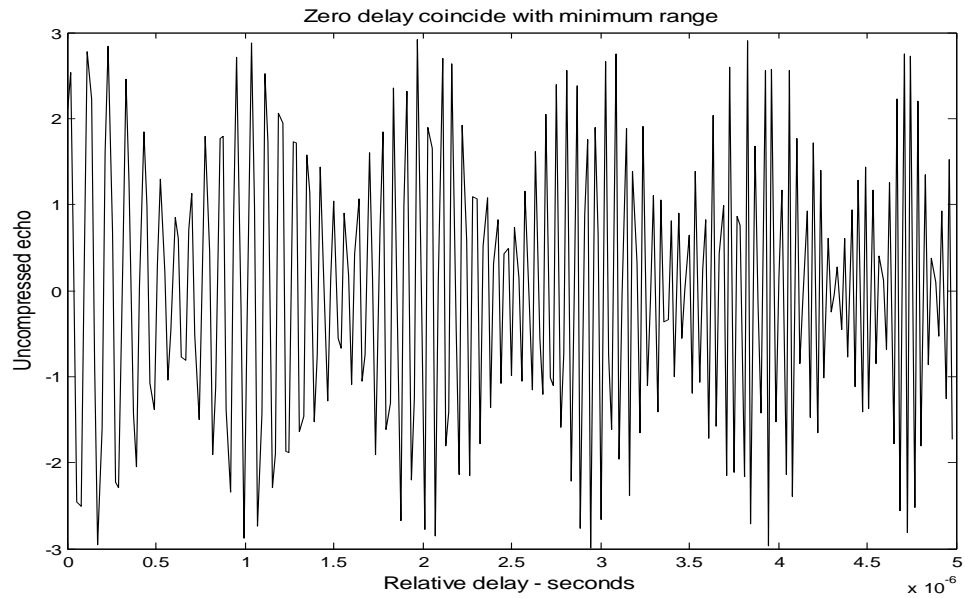


Figure 4.5. Uncompressed echo signal. Scatterers are unresolved

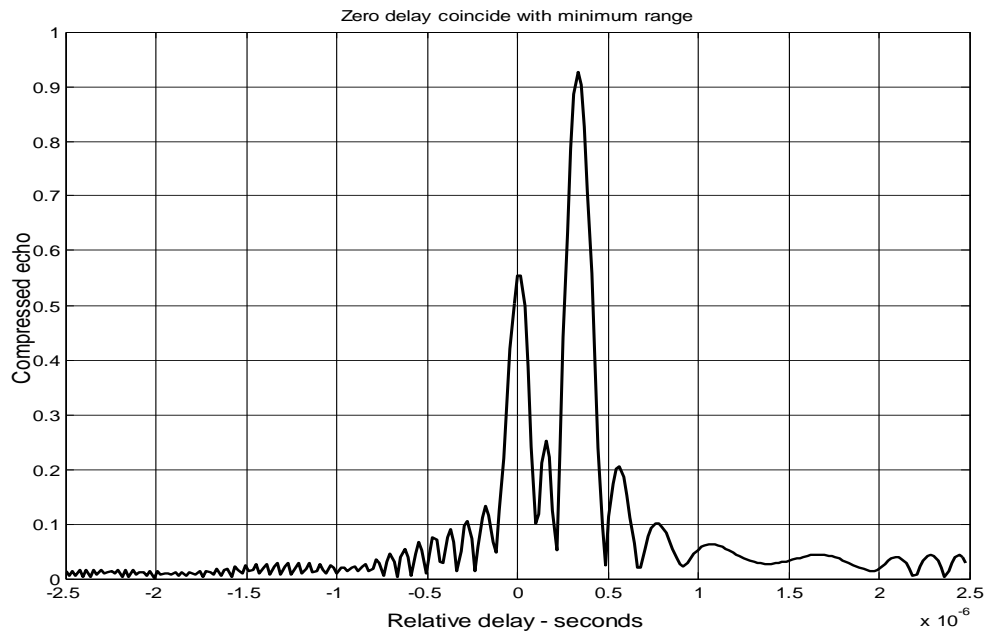


Figure 4.6. Compressed echo signal. Scatterers are resolved

4.4.2. Stretch Processor

Stretch processing, also known as “active correlation,” is normally used to process extremely high bandwidth LFM waveforms. This processing technique consists of the following steps: First, the radar returns are mixed with a replica (reference signal) of the transmitted waveform. This is followed by Low Pass Filtering (LPF) and coherent detection. Next, Analog to Digital (A/D) conversion is performed; and finally, a bank of Narrow Band Filters (NBFs) is used in order to extract the tones that are proportional to target range, since stretch processing effectively converts time delay into frequency. All returns from the same range bin produce the same constant frequency. Fig. 4.7 shows a block diagram for a stretch processing receiver. The reference signal is an LFM waveform that has the same LFM slope as the transmitted LFM signal. It exists over the duration of the radar “receive-window,” which is computed from the difference between the radar maximum and minimum range. Denote the start frequency of the reference chirp as f_r .

Consider the case when the radar receives returns from a few close (in time or range) targets. Mixing with the reference signal and performing low pass filtering are effectively equivalent to subtracting the return frequency chirp from the reference signal. Thus, the LPF output consists of constant tones corresponding to the targets’ positions. The normalized transmitted signal can be expressed by

$$s_1(t) = \cos\left(2\pi\left(f_o t + \frac{\mu_o}{2}t^2\right)\right) \quad 0 \leq t \leq \tau' \quad (4.14)$$

Where $\mu = B/\tau'$ is the LFM coefficient and is the chirp start frequency f_o . Assume a point scatterer at range R. The received signal by the radar is

$$s_r(t) = a \cos\left[2\pi\left(f_o(t - \Delta\tau) + \frac{\mu}{2}(t - \Delta\tau)^2\right)\right] \quad (4.15)$$

Where ‘a’ is proportional to target RCS, antenna gain, and range attenuation. The time delay $\Delta\tau$ is

$$\Delta\tau = 2R/c \quad (4.16)$$

Assume a radar system using a stretch processor receiver. The pulse width is τ' and the chirp bandwidth is B . Since stretch processing is normally used in extreme bandwidth cases (i.e., very large B), the receive window over which radar returns will be processed is typically limited to few meters to possibly less than 100 meters. The compressed pulse range resolution is computed from Eq. (4.9). Declare the FFT size by N and its frequency resolution by Δf . The frequency resolution can be computed using the following procedure: consider two adjacent point scatterers at range R_1 and R_2 . The minimum frequency separation Δf , between those scatterers so that they are resolved can be computed more precisely,

$$\Delta f = f_2 - f_1 = \frac{2B}{c\tau'}(R_2 - R_1) = \frac{2B}{c\tau'} \Delta R \quad (4.17)$$

Now, substituting Eqn. (4.9) into Eqn. (4.17) yields

$$\Delta f = \frac{2B}{c\tau'} \frac{c}{2B} = \frac{1}{\tau'} \quad (4.18)$$

The maximum resolvable frequency by the FFT is limited to the region $\pm N\Delta f/2$. Thus, the maximum resolvable frequency is

$$\frac{N\Delta f}{2} > \frac{2B(R_{mxm} - R_{mnm})}{c\tau'} = \frac{2BR_{rec}}{c\tau'} \quad (4.19)$$

Using Eqn. (4.18) into Eq. (4.19) and collecting term yields

$$N > 2BT_{rec} \quad (4.20)$$

For better implementation of the FFT, choose an FFT of size

$$N_{FFT} \geq N = 2^m \quad (4.21)$$

Here, m is a non zero positive integral.

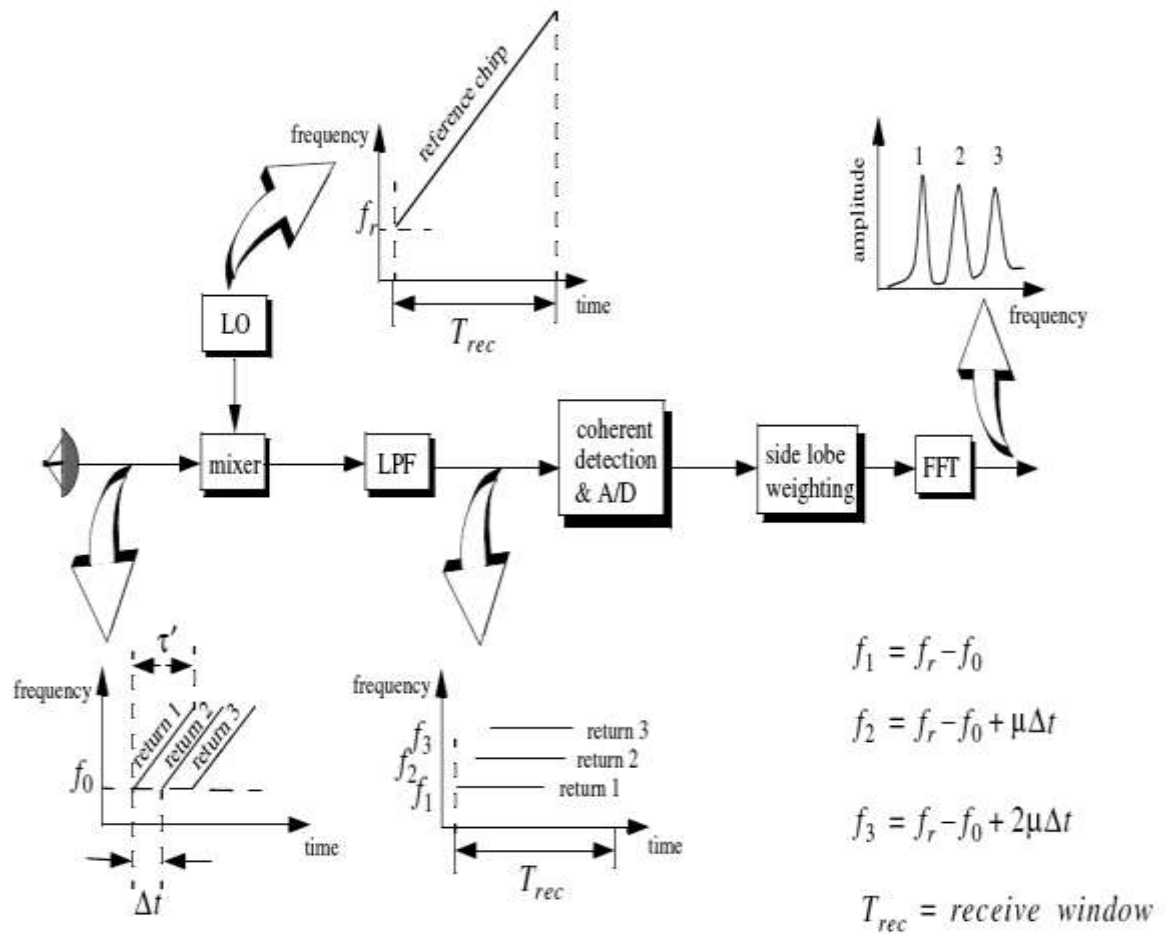


Figure 4.7. Stretch Processor Block Diagram

The sampling interval is then given by

$$\Delta f = \frac{1}{T_s N_{FFT}}$$

$$\text{Or, } T_s = \frac{1}{\Delta f N_{FFT}} \quad (4.22)$$

Fig.4.8 and 4.9, respectively, show the uncompressed and compressed echo signals corresponding to this example by using MATLAB coding.

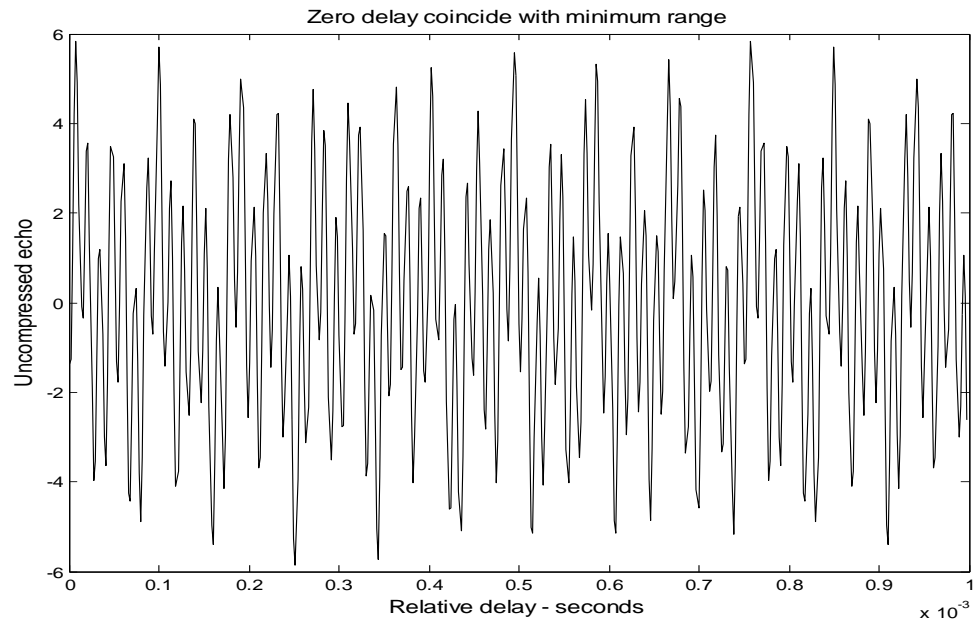


Figure 4.8. Uncompressed echo signal. 3 targets are unresolved

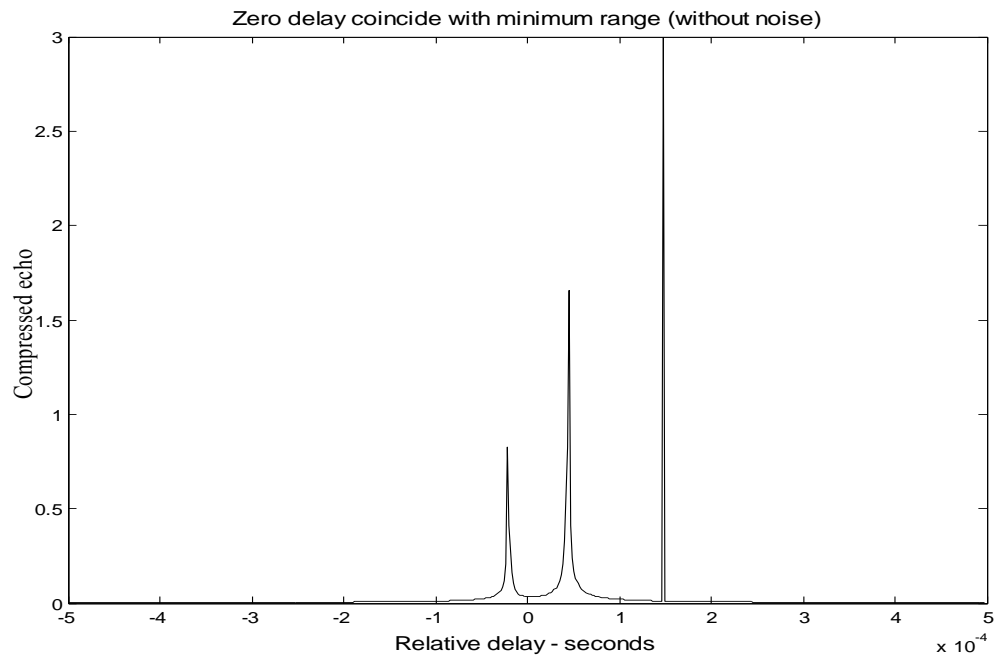


Figure 4.9. Compressed echo signal. 3 targets are resolved

4.4.3. Distortion Due to Target Velocity

We have analyzed pulse compression with no regards to target velocity. In fact, all analyses provided assumed stationary targets. Uncompensated target radial velocity, or equivalently Doppler shift, degrades the quality of the HRR profile generated by pulse compression. The effects of radial velocity on SFW were analyzed; similar distortion in the HRR profile is also present with LFM waveforms when target radial velocity is not compensated for.

When the target radial velocity is not zero, the received pulse width is expanded (or compressed) by the time dilation factor. Additionally, the received pulse center frequency is shifted by the amount of Doppler frequency. When these effects are not compensated for, the pulse compression processor output is distorted. This is illustrated in Fig. 4.10. Fig. 4.10a shows a typical output of the pulse compression processor with no distortion. Alternatively, Figs. 4.10b, 4.10c show the output of the pulse compression processor when 5% shift of the chirp center frequency and 10% time dilation are present.

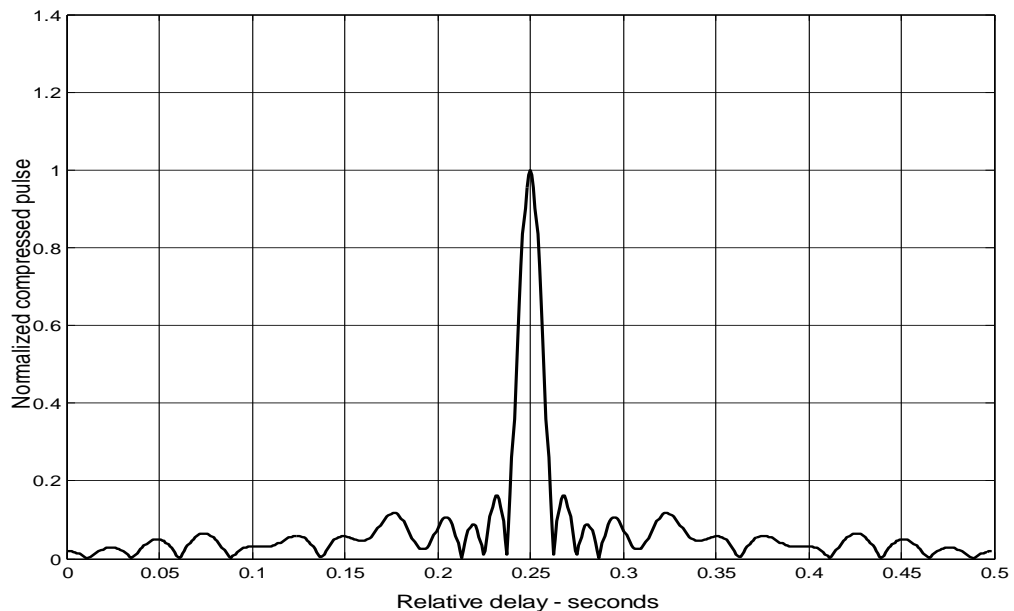


Figure 4.10. (a) Compressed pulse output of a pulse compression processor. No distortion is present.

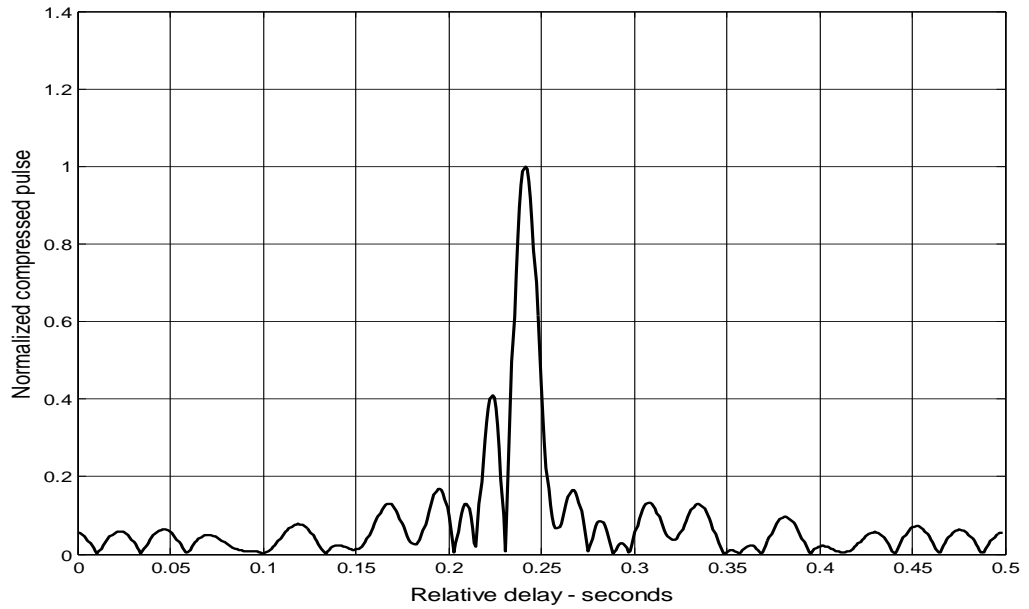


Figure 4.10. (b) Mismatched compressed pulse; 5% Doppler shift.

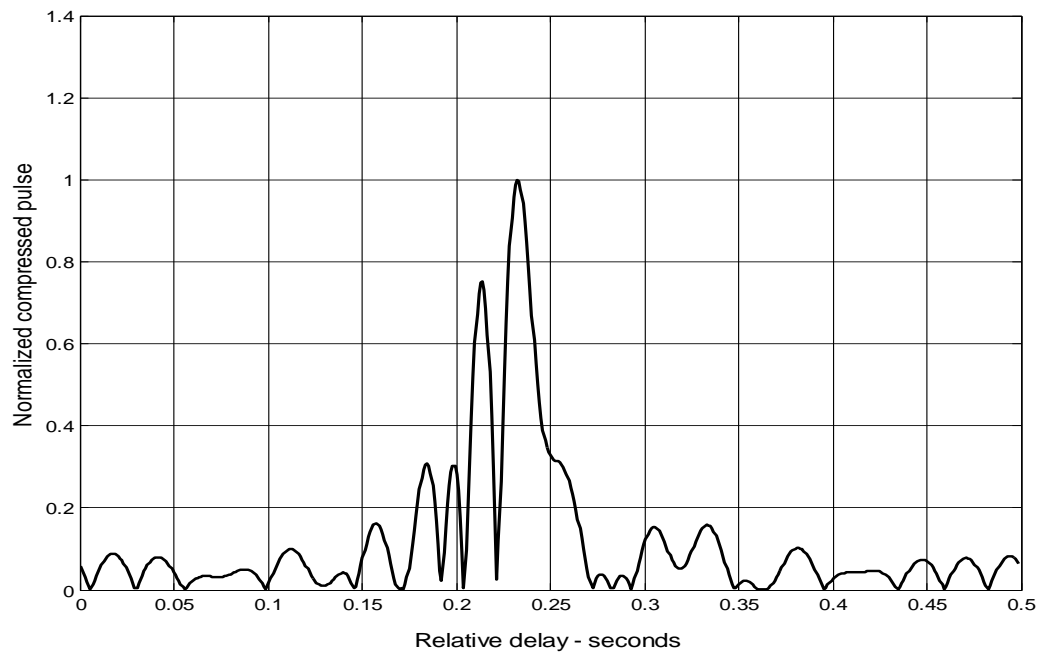


Figure 4.10. (c) Mismatched compressed pulse; 10% time dilation.

4.5. Digital Pulse Compression

In this section we will briefly discuss three digital pulse compression techniques. They are frequency codes, binary phase codes, and poly-phase codes. Costas codes, Barker Codes, and Frank codes will be presented to illustrate, respectively, frequency, binary phase, and poly-phase coding. We will determine the pulse compression goodness of a code, based on its autocorrelation function since in the absence of noise the output of the matched filter is proportional to the code autocorrelation. Given the autocorrelation function of a certain code, the main lobe width (compressed pulse width) and the side lobe levels are the two factors that need to be considered in order to evaluate the code's pulse compression characteristics.

4.5.1. Frequency Coding (Costas Codes)

Construction of Costas codes can be understood from the construction process of Stepped Frequency Waveforms (SFW). In SFW, a relatively long pulse of length τ' is divided into N sub pulses each of width τ_1 ($\tau' = N\tau_1$). Each group of N sub pulses is called a burst. Within each burst the frequency is increased by Δf from one sub pulse to the next. The overall burst bandwidth is $N\Delta f$. More precisely,

$$\tau_1 = \tau' / N \quad (4.23)$$

And the frequency for the i th sub pulse is

$$f_i = f_0 + i\Delta f \quad ; i= 1, N \quad (4.24)$$

Where f_0 is a constant frequency and $f_0 \gg \Delta f$. It follows that the time-bandwidth product of this waveform is

$$\Delta f \tau' = N^2 \quad (4.25)$$

Costas signals (or codes) are similar to SFW, except that the frequencies for the sub pulses are selected in a random fashion, according to some predetermined rule or logic. For this purpose, consider the $N \times N$ matrix shown in Fig. 4.11. In this case, the rows

are indexed from $i = 1, 2, \dots, N$ and the columns are indexed from $j = 0, 1, 2, \dots, (N-1)$. The rows are used to denote the sub pulses and the columns are used to denote the frequency. A “dot” indicates the frequency value assigned to the associated sub pulse. In this fashion, Fig. 4.11a shows the frequency assignment associated with a SFW. Alternatively, the frequency assignments in Fig. 4.11b are chosen randomly. For a matrix of size $N \times N$, there are a total of $N!$ possible ways of assigning the “dots” (i.e., $N!$ Possible codes).

The sequences of “dots” assignment for which the corresponding ambiguity function approaches an ideal or a “thumbtack” response are called Costas codes. A near thumbtack response was obtained by Costas1 by using the following logic: only one frequency per time slot (row) and per frequency slot (column). Therefore, for an $N \times N$ matrix the number of possible Costas codes is drastically less than $N!$. For example, there are $N_c = 4$ possible Costas codes for $N = 3$, and $N_c = 40$ possible codes for $N = 5$. It can be shown that the code density, defined as the ratio $N_c/N!$, significantly gets smaller as N becomes larger.

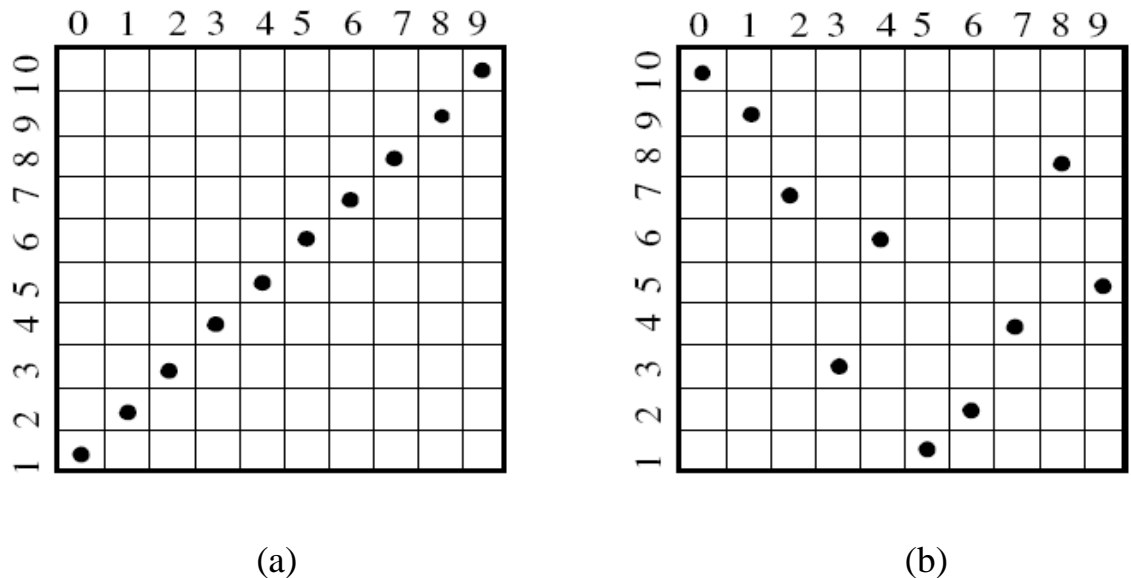


Figure 4.11. Frequency assignment for a burst of N sub pulses. (a) SFW (stepped LFM);(b)Costas code of length $N_c = 10$.

There are numerous analytical ways to generate Costas codes. In this section we will describe two of these methods. First, q let be an odd prime number, and choose the number of sub pulses as

$$N = q - 1 \quad (4.26)$$

Define γ as the primitive root of q . A primitive root of (an odd prime number) is defined as γ such that the powers $\gamma, \gamma^1, \gamma^2, \dots, \gamma^{q-1}$ modulo q generate every integer from 1 to -1 . We can define the normalized complex envelope of the Costas signal as

$$s(t) = \frac{1}{\sqrt{N\tau_1}} \sum_{l=0}^{N-1} s_l(t - l\tau_1) \quad (4.27)$$

$$s_l(t) = \begin{cases} \exp(2\pi f_1 t) & 0 \leq t \leq \tau_1 \\ 0 & \text{elsewhere} \end{cases} \quad (4.28)$$

Costas showed that the output of the matched filter is

$$\chi(\tau, f_D) = \frac{1}{N} \sum_{l=0}^{N-1} \exp(j2\pi l f_D \tau) \left\{ \phi_{ll}(\tau, f_D) + \sum_{\substack{q=0 \\ q \neq l}}^{N-1} \phi_{lq}(\tau - (l - q)\tau_1, f_D) \right\} \quad (4.29)$$

$$\phi_{lq}(\tau, f_D) = \left(\tau - \frac{|\tau|}{\tau_1} \right) \frac{\sin \alpha}{\alpha} \exp(-j\beta - j2\pi f_q \tau) \quad (4.30)$$

Three-dimensional plots for the ambiguity function of Costas signals show the near thumbtack response of the ambiguity function. All side lobes, except for few around the origin, have amplitude $1/N$. Few side lobes close to the origin have amplitude $2/N$, which is typical of Costas codes. The compression ratio of a Costas code is approximately N .

4.5.2. Binary Phase Code

In this case, a relatively long pulse of width τ' is divided into N smaller pulses; each is of width $\Delta\tau = \tau'/N$. Then, the phase of each sub-pulse is randomly chosen as either 0

or π radians relative to some CW reference signal. It is customary to characterize a sub-pulse that has 0 phase (amplitude of +1 Volt) as either “1” or “+.” Alternatively, a sub-pulse with phase equal to π (amplitude of -1 Volt) is characterized by either “0” or “-.” The compression ratio associated with binary phase codes is equal to $\xi = \tau' / \Delta\tau$, and the peak value is N times larger than that of the long pulse. The goodness of a compressed binary phase code waveform depends heavily on the random sequence of the phase for the individual sub-pulses.

One family of binary phase codes that produce compressed waveforms with constant side lobe levels equal to unity is the Barker code. Fig. 4.12 illustrates this concept for a Barker code of length seven. A Barker code of length n is denoted as B_n . There are only seven known Barker codes that share this unique property; they are listed in Table 4.1. Note that B_2 and B_4 have complementary forms that have the same characteristics. Since there are only seven Barker codes, they are not used when radar security is an issue.

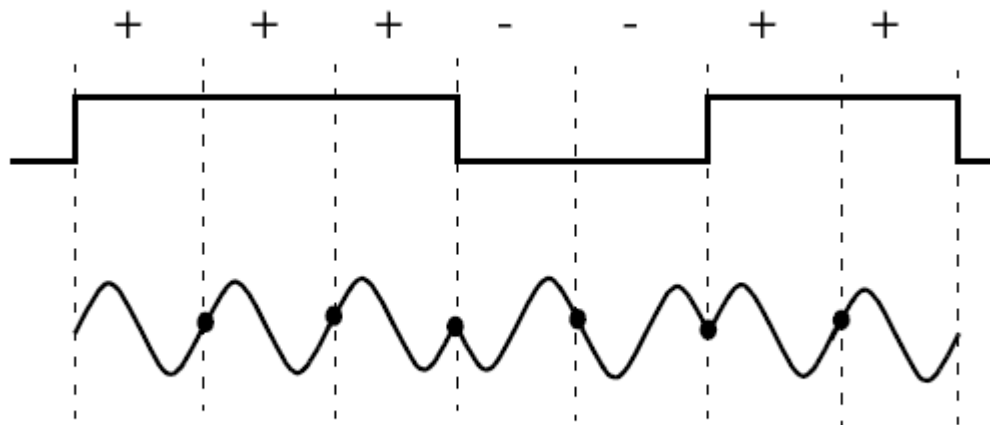


Figure 4.12. Binary phase code of length 7.

Table 4.1. Barker Codes

Code symbol	Code length	Code elements	Side lobe reduction (dB)
B_2	2	+ -	6.0
		++	
B_3	3	++ -	9.5
B_4	4	++ - +	12.0
		+++ -	
B_5	5	+++ - +	14.0
B_7	7	+++ - - + -	16.9
B_{11}	11	+++ - - - + - - + -	20.8
B_{13}	13	+++++ - - + + - + - +	22.3

In general, the autocorrelation function (which is an approximation for the matched filter output) for a B_N Barker code will be $2N\Delta\tau$ wide. The main lobe is $2\Delta\tau$ wide; the peak value is equal to N . There are $(N - 1)/2$ side lobes on either side of the main lobe; this is illustrated in Fig. 4.13 for a B_{13} . Notice that the main lobe is equal to 13, while all side lobes are unity.

The most side lobe reduction offered by a Barker code is -22.3 dB , which may not be sufficient for the desired radar application. However, Barker codes can be combined to generate much longer codes. In this case, a B_m code can be used within a B_n code (m within n) to generate a code of length mn . The compression ratio for the combined B_{mn} code is equal to mn . As an example, a combined is given by

$$B_{54} = \{ 11101, 11101, 00010, 11101 \} \quad (4.31)$$

and is illustrated in Fig. 4.14. Unfortunately, the side lobes of a combined Barker code autocorrelation function are no longer equal to unity. Some side lobes of a Barker code autocorrelation function can be reduced to zero if the matched filter is followed by a linear transversal filter with impulse response given by

$$h(t) = \sum_{k=-N}^N \beta_k \delta(t - 2k\Delta\tau) \quad (4.32)$$

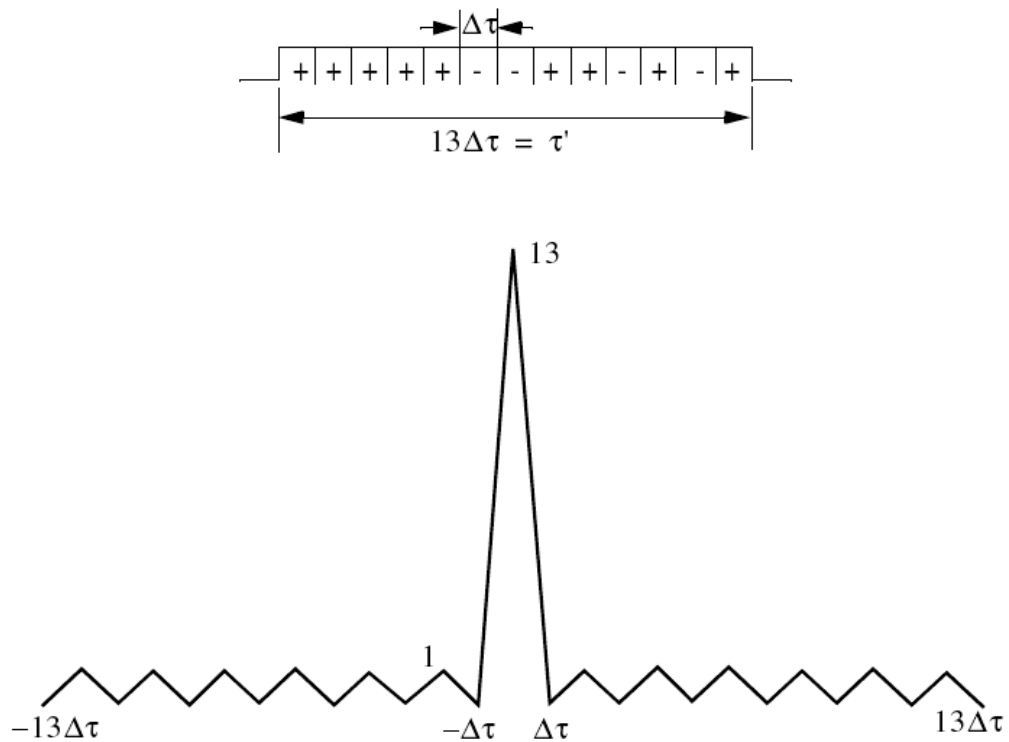


Figure 4.13. Barker code of length 13, and its corresponding autocorrelation function.

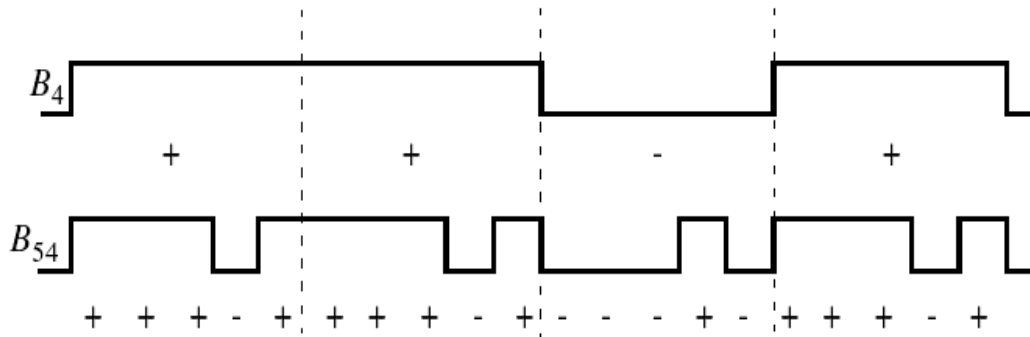


Figure 4.14. A combined B_{54} Barker code

Where N is the filter's order, the coefficients β_k ($\beta_k = \beta_{-k}$) are to be determined, $\delta(\bullet)$ is the delta function, and τ is the Barker code sub-pulse width. A filter of order N produces zero side lobes on either side of the main lobe. The main lobe amplitude and width do not change. This is illustrated in Fig. 4.15.

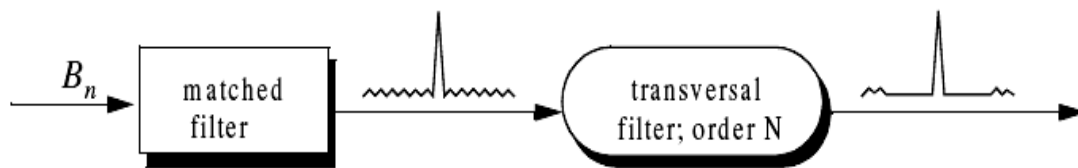


Figure 4.15. A linear transversal filter of order N can be used to produce N zero side lobes in the autocorrelation function. In this figure, $N = 4$.

4.5.3. Frank Codes

Codes that use any harmonically related phases based on a certain fundamental phase increment are called poly-phase codes. We will demonstrate this coding technique using Frank codes. In this case, a single pulse of width τ' is divided into N equal groups; each group is subsequently divided into other N sub-pulses each of width $\Delta\tau$. Therefore, the total number of sub-pulses within each pulse is N^2 , and the compression ratio is $\xi =$

N^2 . As before, the phase within each sub-pulse is held constant with respect to some CW reference signal.

A Frank code of N^2 sub-pulses is referred to as an N-phase Frank code. The first step in computing a Frank code is to divide 360° by N , and define the result as the fundamental phase increment $\Delta\phi$. More precisely,

$$\Delta\phi = \frac{360^\circ}{N} \quad (4.33)$$

The size of the fundamental phase increment decreases as the number of groups is increased, and because of phase stability, this may degrade the performance of very long Frank codes. For N-phase Frank code the phase of each sub-pulse is computed from

$$\begin{pmatrix} 0 & 0 & 0 & 0 & \cdots & 0 \\ & & \vdots & & \ddots & \vdots \\ 0 & N-1 & 2(N-1) & 3(N-1) & \cdots & (N-1)^2 \end{pmatrix} \quad (4.34)$$

Where each row represents a group, and a column represents the sub-pulses for that group. For example, a 4-phase Frank code has $N = 4$, and the fundamental phase increment is $\Delta\phi = 360^\circ/4 = 90^\circ$

Therefore, a Frank code of 16 elements is given by

$$F_{16} = \{ 1 \ 1 \ 1 \ 1 \ 1 \ j \ -1 \ -j \ 1 \ -1 \ 1 \ -1 \ 1 \ -j \ -1 \ j \} \quad (4.35)$$

The phase increments within each row represent a stepwise approximation of an up-chirp LFM waveform. The phase increments for subsequent rows increase linearly versus time. Thus, the corresponding LFM chirp slopes also increase linearly for subsequent rows. This is illustrated in Fig. 4.16, for F_{16} .

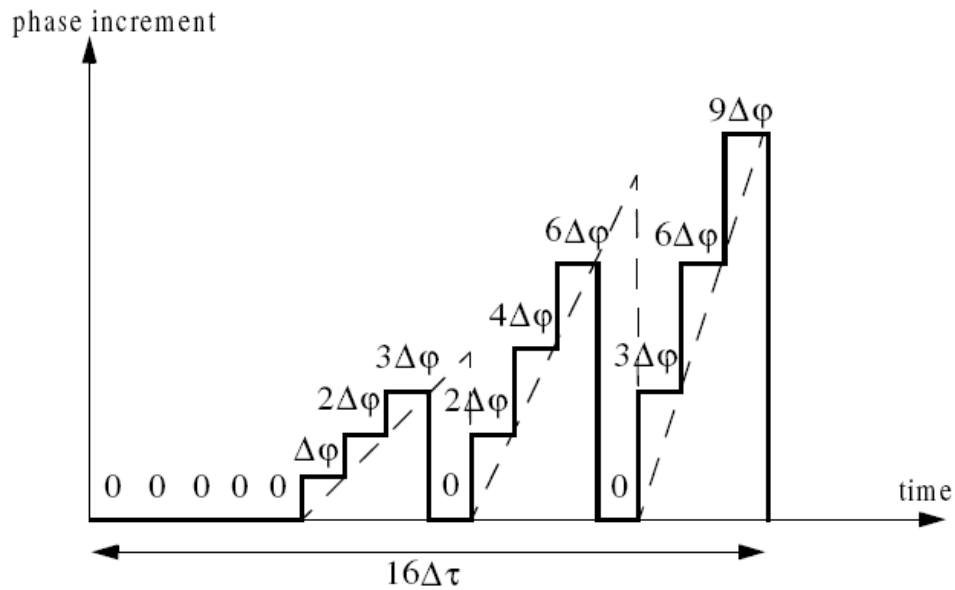


Figure 4.16. Stepwise approximation of an up-chirp waveform using a Frank code of 16 elements.

4.5.4. Pseudo-Random (PRN) Codes

Pseudo-random (PRN) codes are also known as Maximal Length Sequences (MLS) codes. These codes are called pseudo-random because the statistics associated with their occurrence is similar to that associated with the coin-toss sequences. Maximum length sequences are periodic with period L and the code values take on two binary values (+1 and -1). The MLS correlation function is

$$\phi(n) = \begin{cases} L & n = 0, \pm L, \pm 2L, \dots \\ -1 & \text{elsewhere} \end{cases} \quad (4.36)$$

Fig. 4.17 shows a typical sketch for an MLS autocorrelation function. Clearly these codes have the advantage that the compression ratio becomes very large as the period is increased.

Additionally, adjacent peaks (grating lobes) become farther apart. Maximum length sequences exist for all integer values m , with a period equal to $2^m - 1$. They can be

generated using shift register circuits with the proper feedback connections, where the sum is a modulo-2 operation. This is illustrated in Fig. 4.18 for $m = 4$ (i.e., $L = 15$). Note that the circuit shown in Fig. 4.18 is not the only one that can produce this code.

In radar applications, long codes are very desirable. However, having very long codes presents many possibilities for the feedback connections through the modulo-2 adder. For example, for $m=80$, the period is $L = 2^{80} - 1$, which is very huge and may take years to produce the corresponding code. Therefore, there is a need for a more systematic method for producing MLS codes.

In practice, typical MLS codes are produced by using the primitive polynomials with the proper degree that corresponds to the code, and the feedback connections are made according to the chosen polynomial, as illustrated in Fig.4.18 for $m = 4$. In this example the primitive polynomial is $x^4 + x + 1$. Of course the initial loading for the registers must be different from all zeros. More details on primitive polynomials can be found in many cited references.

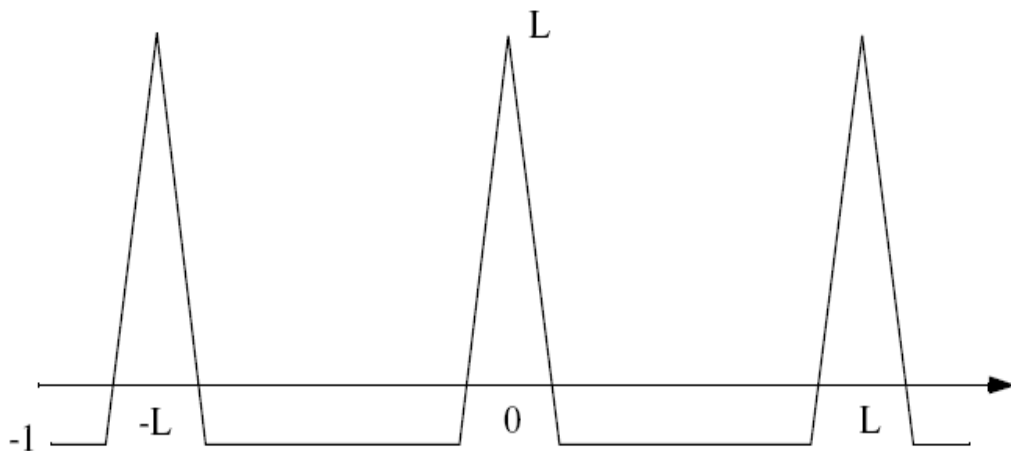


Figure 4.17. Typical correlation of an MLS code of length L

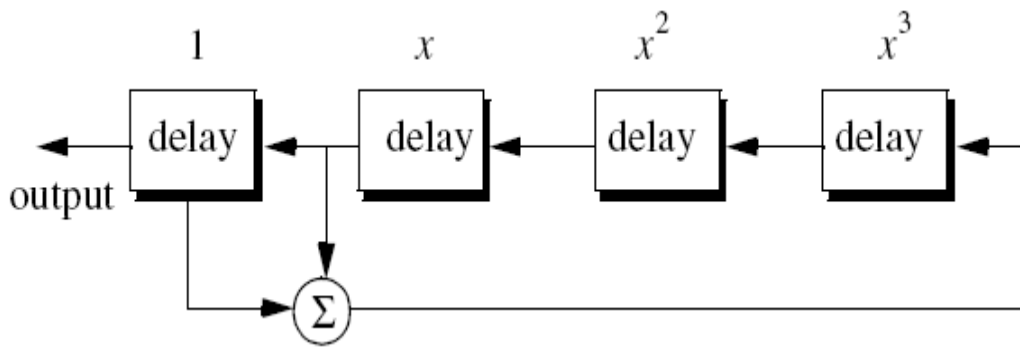


Figure 4.18. Circuit for generating an MLS sequence of length $L = 15$

The primitive polynomial is $x^4 + x + 1$

Chapter 5

COMPARATIVE STUDY AMONG DIFFERENT PULSE COMPRESSION TECHNIQUE

5.1. Introduction

Reduction in the peak power of a pulse can be achieved by increasing the length of the Pulse. But, an increase in the length of the pulse reduces range resolution. To avoid the compromise in range resolution, some form of encoding must be done within the transmitted pulse, so that it is possible to "compress" a longer pulse into a shorter one in the receiver using suitable signal processing operations. The easiest form of such encoding is to allow the radar pulse to modulate a waveform or a sequence that is uncorrelated in time but known at the receiver. A cross-correlation operation at the receiver (using the known transmitted waveform/sequence) will compress the long received waveform/sequence into a short one. This is due to the time auto-correlation properties of the transmitted waveform/sequence, which is maximum at zero-lag and almost zero at lags other than zero. Another important effect of Pulse Compression is the increase in the bandwidth of the signal. Without Pulse Compression, a longer pulse has a lesser bandwidth than a shorter pulse. But, due to the encoding associated with Pulse Compression, the bandwidth of the longer pulse increases. In fact, to have higher range resolution using pulse compression, the waveform/sequence encoding should be highly uncorrelated and thus use a larger band-width. The objective of designing a good Pulse Compression scheme is now to choose an encoding signal that has a very narrow auto-correlation function.

5.2. Simulation of Different Pulse compression

Simulation has been carried out for analog and digital pulse compression technique using MATLAB software. For the compression we have used chirp frequency of 5.6

GHz and chirp bandwidth of 1GHz. Scattering range of 150 km is also used. In the simulation we vary the weighting function and show the corresponding output and finally compare the outputs. As we have used MATLAB software, for simulation we have to fix some parameters which are suitable and easy to simulate and which do not exceed the range. It should be noted that the compressed pulse range resolution is $\Delta R = 0.15 \text{ m}$

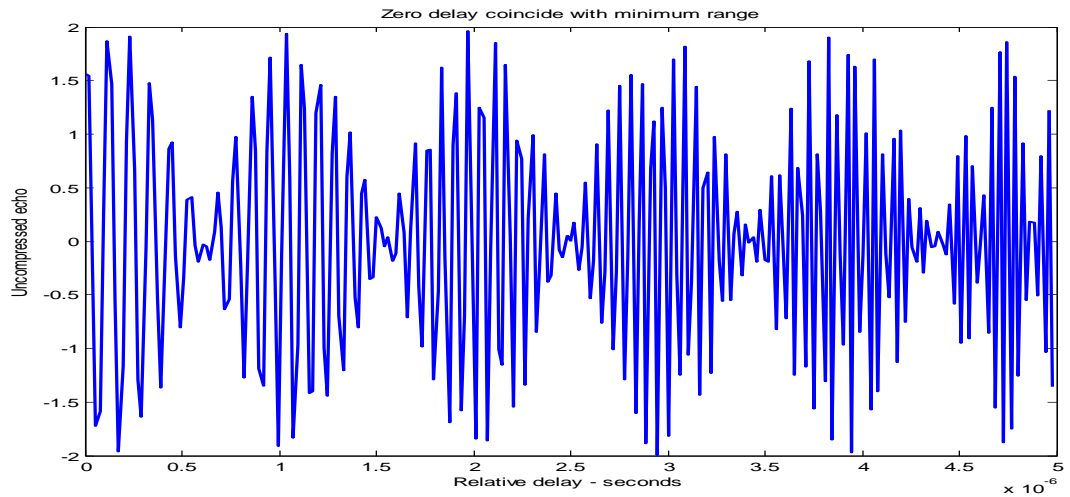


Figure 5.1. Uncompressed Echo of Received Signal

5.2.1. Pulse compression Using Matched Filter

Output of a matched filter is just the correlation of the received signal with a delayed version of the transmitted signal. In the FMCW case this function is implemented by taking the product of the received signal with the transmitted signal and filtering to obtain a constant frequency beat, as discussed. The spectrum is then determined using the Fourier transform or a similar spectral estimation process.

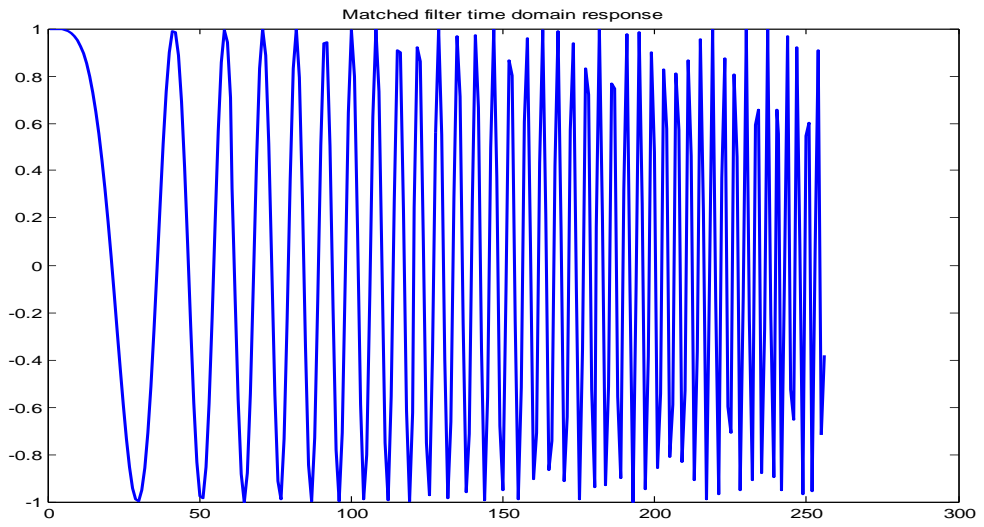


Figure 5.2. Matched filter time domain response

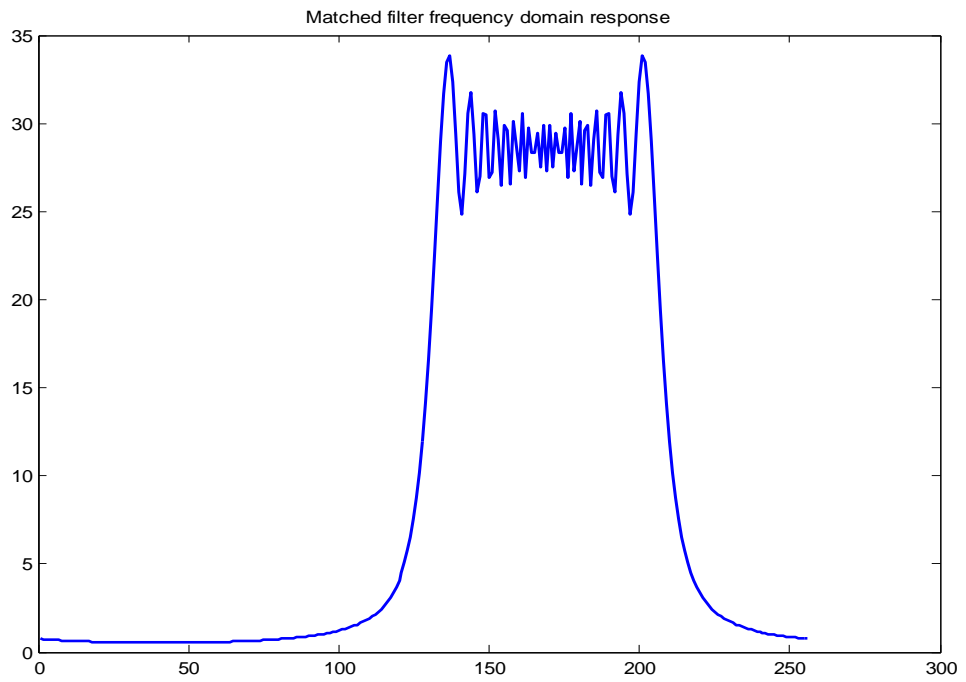


Figure 5.3. Matched filter frequency domain response

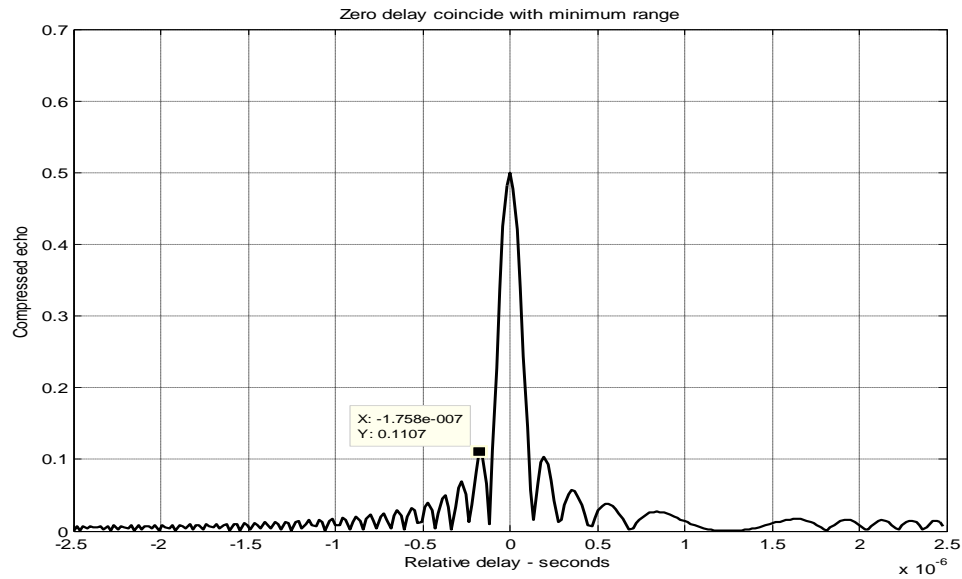


Figure 5.4. Compressed echo of received signal using no weighting function

5.2.1.1. Window Variation over matched filter response

Weighting functions (windows) can be used on the compressed pulse spectrum in order to reduce the side lobe levels. The cost associated with such an approach is a loss in the main lobe resolution, and a reduction in the peak value. Weighting the time domain transmitted or received signal instead of the compressed pulse spectrum will theoretically achieve the same goal. However, this approach is rarely used, since amplitude modulating the transmitted waveform introduces extra burdens on the transmitter. We compare the performance of different side lobe reduction technique varying different windows. Hamming, Kaiser and Chebyshev window are used to show the comparison.

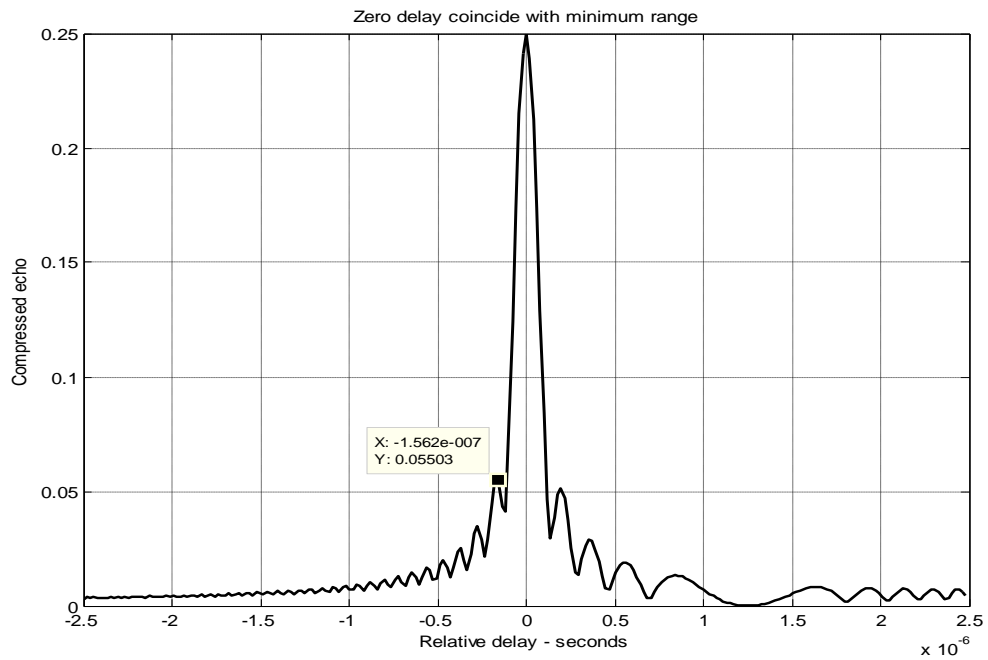


Figure 5.5. (a) Compressed echo of received signal using hamming weighting function

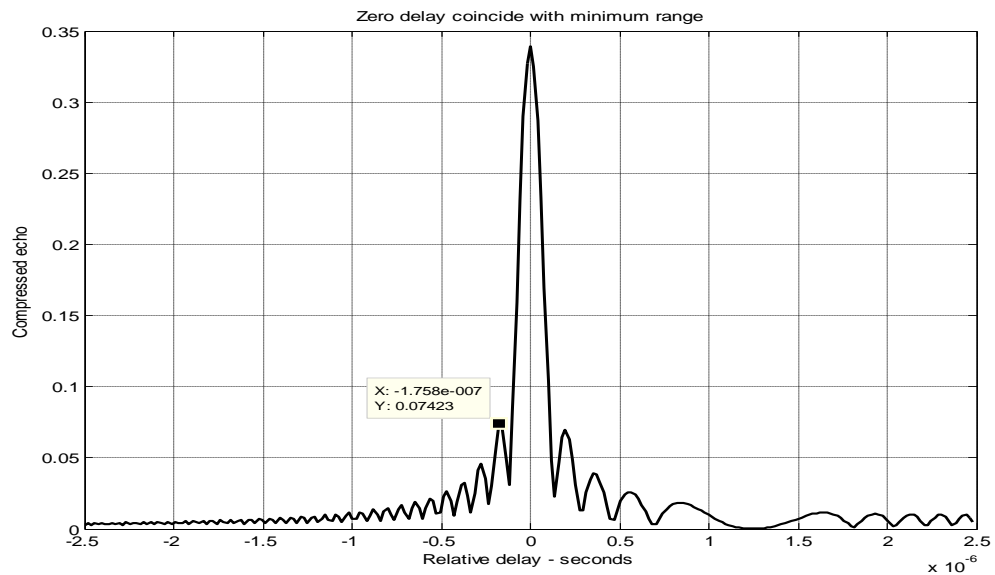


Figure 5.5. (b) Compressed echo of received signal using Kaiser weighting function

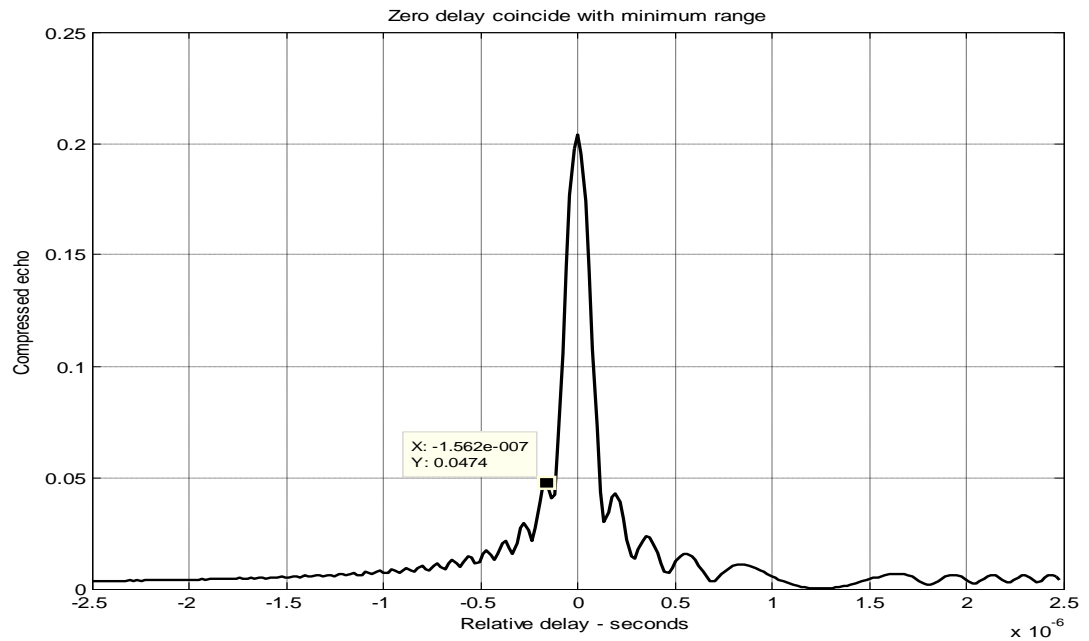


Figure 5.5. (c) Compressed echo of received signal using chebyshev weighting function

5.2.2. Stretch Processor

In Stretch a linear FM pulse is transmitted and then the return echo is demodulated by down converting using a frequency modulated LO signal of identical or slightly different FM slope. If the identical slope is used then the echo spectrum corresponds to the range profile. This is a form of pulse compression intermediate between standard pulse compression and FMICW. If the slope of the LO is different to that of the transmitted chirp, then the output of the Stretch processor comprises signals with a reduced chirp. These can then be processed using a standard SAW pulse compression system to produce target echoes as described in the previous section.

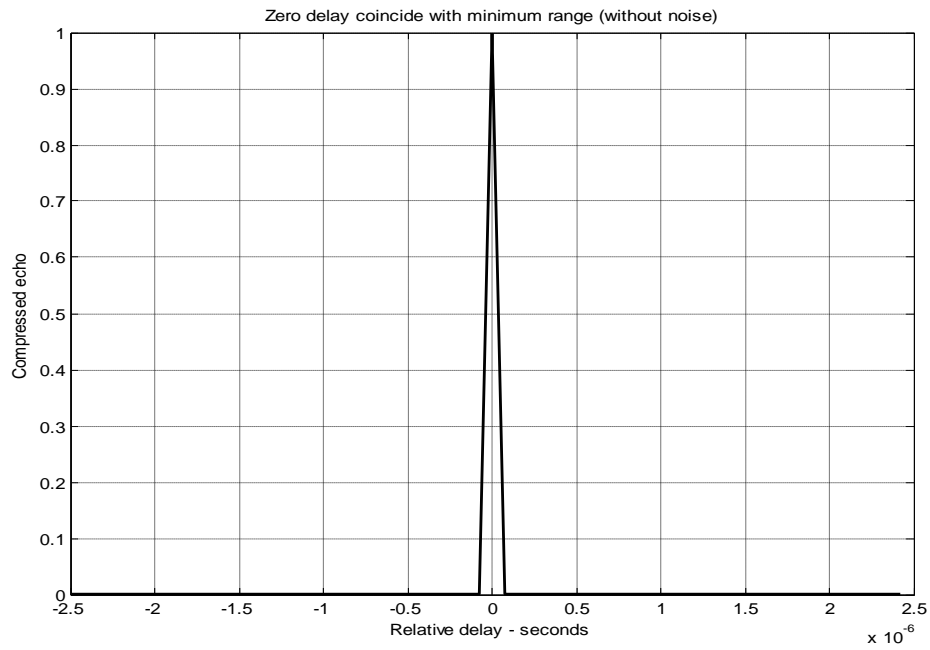


Figure 5.6. (a) Compressed echo for single target using stretch processing technique

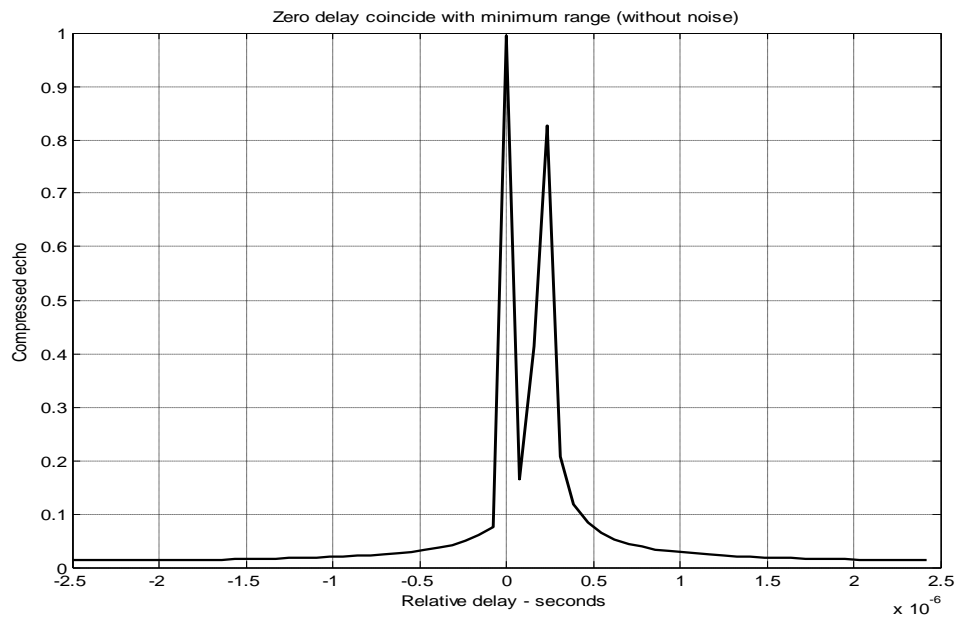


Figure 5.6. (b) Compressed echo for two targets using stretch processing technique

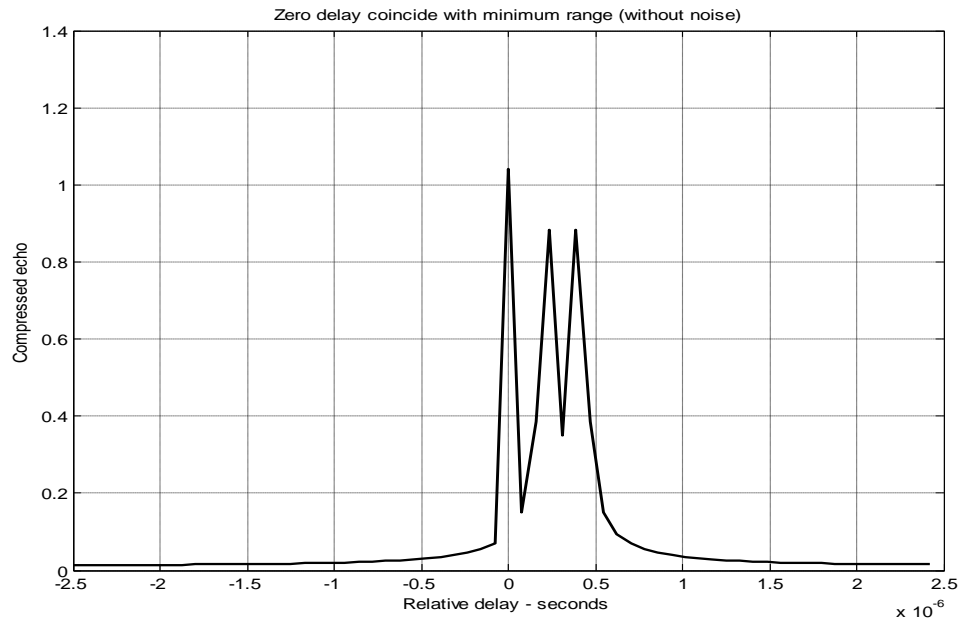


Figure 5.6. (c) Compressed echo for three targets using stretch processing technique

5.2.3 Digital Pulse Compression

Barker Code is used here as digital pulse compression. Barker Code of different lengths is used here for multiple targets.

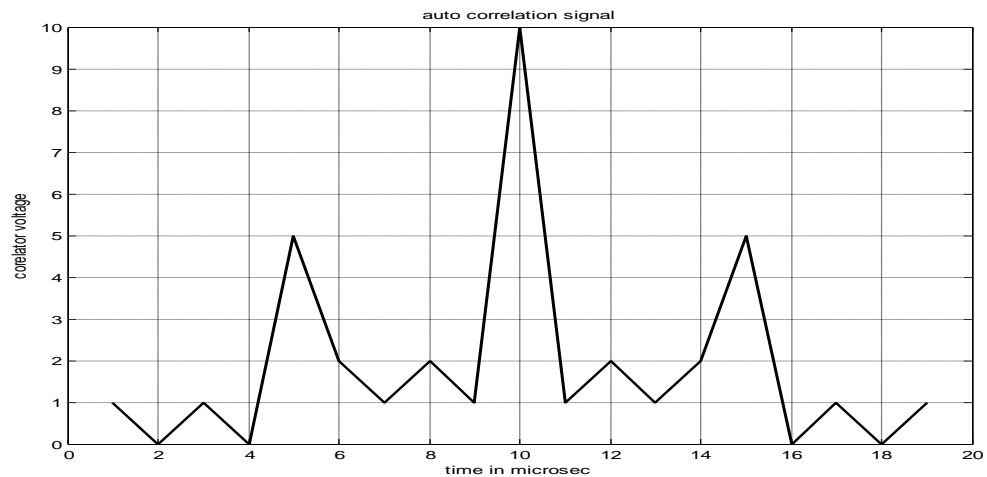


Figure 5.7. (a) Digital pulse compression technique using Barker Code of length five (B_5) for three targets

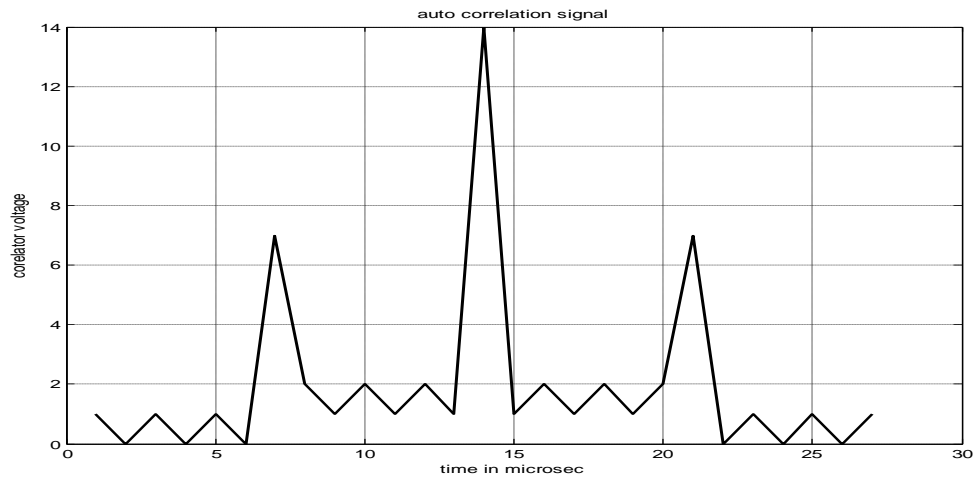


Figure 5.7. (b) Digital pulse compression technique using Barker Code of length seven (B_7) for three targets

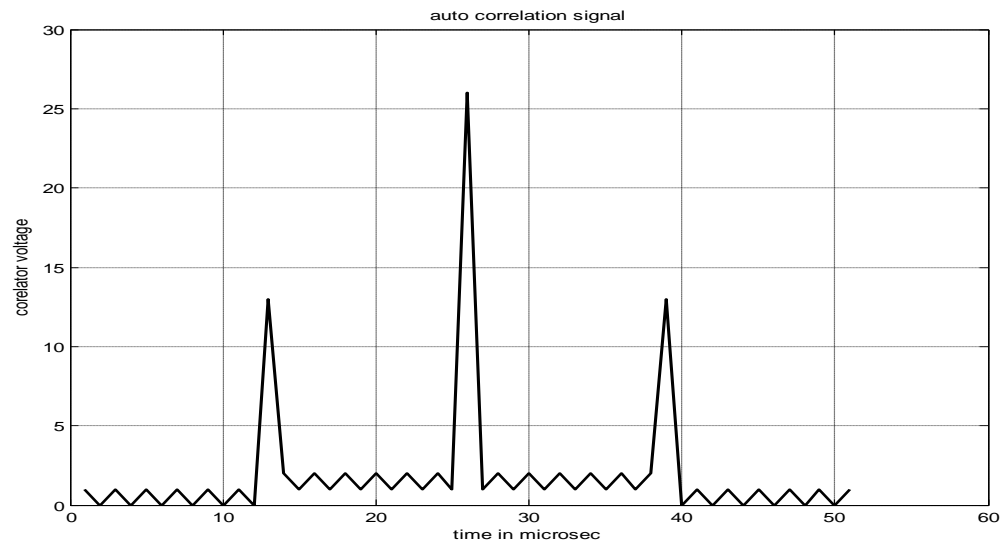


Figure 5.7. (c) Digital pulse compression technique using Barker Code of length thirteen (B_{13}) for three targets

5.3. Result and Discussion on Simulation

To compare the performance of different pulse compression technique we instruct them to track the same target with varying weighting function for pulse compression using matched filter. We have plotted the compressed echo varying weighting function in figure 5.5. For stretch processor and digital pulse compression we referred them to track multiple targets. We checked the delectability of compressed echo for multiple targets in figure 5.6 and figure 5.7. First Side lobe Ratio (SLR) for compressed echo for different pulse compression technique is listed below

Table 5.1. First side lobe Ratio (SLR) for different pulse compression technique

Name of Process	First side lobe Ratio (SLR) in db
Matched filter with no window	-13.09
Matched filter with Hamming window	-13.14
Matched filter with Kaiser window	-13.46
Matched filter with Chebyshev window	-12.92
Stretch Processor for single target	Tensed to minus infinity
Barker Code of length five(B_5)	-13.97
Barker Code of length seven(B_7)	-16.90
Barker Code of length thirteen(B_{13})	-22.27

For multiple targets there is no overlapping of main lobes for Digital Pulse compression (figure 5.7). For stretch processor technique two main lobes overlap each other (Figure 5.6(b) & 5.6(c)).

Chapter 6

CONCLUSION AND FUTURE WORKS

6.1. Results and Discussions

Chapter 1 begins with the basic radar system, its origination and classification along with the operating frequency bands. In the process, it is shown graphically that increasing the pulse width increases the effective detection range for a pulsed radar system. It is not an economic way to increase the range as it means increasing the transmitted power. However,, fine resolution requires pulse width to be as small as possible (or bandwidth as large as possible). Achieving fine range resolution while maintaining adequate average transmitted power can be accomplished by using pulse compression techniques (not part of this thesis).

In chapter 2, the basic equation for a monostatic pulsed radar system is developed. The analysis was extended to find the equation for the bistatic radar system. Then different parameters were varied to observe their effects on the radar range by using MATLAB simulation. Doubling the peak power improves SNR only a little where as doubling the RCS improves SNR a little better. Other radar parameters such as antenna gain variation should be considered to improve SNR or detection range effectively. Integrating a limited number of pulses can significantly enhance the SNR. However, integrating large amount of pulses does not provide any further major improvement in radar performance. We also found from the simulation that we can increase the antenna aperture to compensate for the lack of power being transmitted to cover a wider range of area for target detection.

In chapter 3, concentration is given on fundamentals of pulse compression. It is shown that the easiest form of pulse compression is to allow the radar pulse to modulate a waveform or sequence that is uncorrelated in time but known at the receiver. A cross-correlation operation at the receiver (using the known transmitted waveform/sequence) will compress the long received waveform/sequence into a short one. This is due to the time auto-correlation properties of the transmitted waveform/sequence, which is maximum at zero-lag and almost zero at lags other than zero. Different weighting functions are discussed here to improve the detection capability of radar while using compressed pulse.

In chapter 4, different types of pulse compression techniques are discussed. It has been shown that how high range resolution depends on pulse compression. Using pulse compression radar can achieve the energy of a long pulse and the resolution of a short-pulse without the high peak power required of a high energy short-duration pulse. For a given set of radar parameters, and as long as the transmitted pulse remains unchanged, then the SNR is also unchanged regardless of the signal bandwidth. Since the spectral bandwidth of a pulse is inversely proportional to its width, the bandwidth of a short pulse is large. Large width can increase system complexity. Here we try to identify suitable pulse compression technique to increase the range resolution having less system complexity. We have also discussed about different types of distortion occurs during pulse compression and try to find out way to avoid distortions during pulse compression.

In chapter 5, a comparison study of different pulse compression techniques is shown by simulating in MATLAB. When we simulate pulse compression using matched filter for single target there arise side lobes. To reduce side lobes we have used different weighting functions. By using stretch processing technique for same target side lobes are totally eradicated. But problem arises when multiple targets are used. Simulation shows that for two or more targets, compressed pulses overlapped each other. It can cause serious limitations on the performance of radars and their ability to perform adequate

target detection. Barker Code of different lengths is simulated here for multiple targets. And the problem of overlapping of two or more compressed pulse is reduced.

As Barker Code of length thirteen (B_{13}) has no overlapping problem and has comparatively lower First Side lobe Ratio (-22.27 DB), it will be 'the best estimated pulse compression technique'.

6.2. Scope of Future Works

The thesis work mostly deals with different pulse compression techniques to improve range resolution for detecting multiple targets. Barker Code of length thirteen (B_{13}) has shown very good performance while simulating for multiple targets. But it still has some side lobes and that can create problem for detecting targets of very weak reflected echo signal. Future works may focus on reducing side lobes for the targets of long distances.

BIBLIOGRAPHY

- [1] Merrill I. Skolnik, "Introduction to Radar Systems", 3rd edition, Tata McGraw-Hill, 2001.
- [2] Bassem R. Mahafza, "Radar Systems Analysis and Design Using MATLAB", 2nd ed, Chapman and Hall/CRC, 2005.
- [3] Simon Haykin, "Communication Systems", 4th edition, John Wiley & Sons, pp. 107 ~ 119, 2000.
- [4] Lambert M. Surhone, Mariam T. Tennoe, Susan F. Henssonow, "Pulse Compression", Betascript Publishing .
- [5] F. E. Nathanson, "Radar Design Principles", 2nd edition, Prentice Hall of India, 1999.
- [6] Marvin N. Cohen. , " Principle of Modern Radar" 1st ed, Springer US, 1987
- [7] David Knox Barton, "Pulse Compression, RADARS Volume 3", 1st ed, Artech House, 1974
- [8] August W. Rihaczek, "Principles of High Resolution Radars" ,Artech House Publishers,1996
- [9] Babak Nikfal, Shulabh Gupta, Christophe Caloz, "Low-Cost Analog Pulse Compression Technique Based on Mixing With an Auxiliary Pulse", IEEE microwave and wireless component letters, vol 22, No. 3, March 2012.
- [10] H. A. Krichene, M. J. Pekala, M. D. Sharp, K. C. Lauritzen, D. G. Lucarelli, and I-J. Wang, "Compressive Sensing and Stretch Processing" IEEE Trasaction 2011

APPENDIX

MATLAB Codes Used for Simulations

A-1 Code for figure 4.11.(a), 4.11.(b) & 4.11.(c)

```
clc
clear all
eps = 1.5e-5;
t = 0:0.001:.5;
y = chirp(t,0,.25,20);
%chirp signal generation
figure(1)
plot(t,y);
yfft = fft(y,512);
rt=abs(ifft(yfft .* conj(yfft)));
ycomp = fftshift(abs(ifft(yfft .* conj(yfft))));
%normalized compressed pulse
maxval = max (ycomp);
ycomp = eps + ycomp ./ maxval;
figure(2)
del = .5 /512.;
tt = 0:del:.5-eps;
%relative delay
plot (tt,ycomp,'k')
%compressed pulse output without any distortion
xlabel ('Relative delay - seconds');
ylabel('Normalized compressed pulse')
grid
%change center frequency
```

```

y1 = chirp (t,0,.25,21);
y1fft = fft(y1,512);
y1comp = fftshift(abs(ifft(y1fft .* conj(yfft))));
maxval = max (y1comp);
y1comp = eps + y1comp ./ maxval;
%normalized compressed pulse
figure(3)
plot (tt,y1comp,'k')
%mismatched compressed pulse with 5% Doppler shift
xlabel ('Relative delay - seconds');
ylabel('Normalized compressed pulse')
grid %change pulse width
t = 0:0.001:.45;
y2 = chirp (t,0,.225,20);
y2fft = fft(y2,512);
y2comp = fftshift(abs(ifft(y2fft .* conj(yfft))));
%normalized compressed pulse
maxval = max (y2comp);
y2comp = eps + y2comp ./ maxval;
figure(4);
plot (tt,y2comp,'k');
%mismatched compressed pulse with 10% time dillation
xlabel ('Relative delay - seconds');
ylabel('Normalized compressed pulse')
grid

```

MATLAB function “power_integer_2.m”

```

function n = power_integer_2 (x)
m = 0.;
for j = 1:30

```

```

m = m + 1.;
delta = x - 2.^m;
if(delta < 0.)
n = m;
return
else
end
end
end

```

A-2 Code for figure 5.1, 5.2 & 5.3

```

clc
clear all
nscat=1; %Number of point scatterers within the received
window
rmin=150000; %Minimum range of receive window
rrec=200; %Receive window size
taup=.000005;%Uncompressed pulse width
f0=14e+6; %Chirp start frequency
b=16e+6;%Chirp bandwidth
scat_range=rmin+[0 25 50];%Vector of scatterers range
scat_rcs=[1 1 1]; %Vector of scatterers RCS
winid=0; %window function
eps = 1.0e-16;
htau = taup/2.;
c = 3.e8;
n = fix(2. * taup * b);
m = power_integer_2(n); %power_integer_2 calling function
nfft = 2.^m;
x(nscat,1:nfft) = 0.;
y(1:nfft) = 0.;
replica(1:nfft) = 0.;
if( winid == 0.)

```

```

win(1:nfft) = 1.;
win =win';
else
if(winid == 1.)
win = hamming(nfft); %hamming window function
else
if( winid == 2.)
win = kaiser(nfft,pi); %kaiser window function
else
if(winid == 3.)
win = chebwin(nfft,60); %chebwin window function
end
end
end
end

deltar = c / 2. / b;
max_rrec = deltar * nfft / 2.;
maxr = max(scatter_range) - rmin;
if(rrec > max_rrec | maxr >= rrec )
'Error. Receive window is too large; or scatterers fall
outside window'
break
end

trec = 2. * rrec / c;

deltat = taup / nfft;
t = 0: deltat:taup-eps;
uplimit = max(size(t));
replica(1:uplimit) = exp(i * 2.* pi * (.5 * (b/taup) .*
t.^2));

```

```

figure(1)
subplot(2,1,1)
plot(real(replica)) %matched filter time domain response
title('Matched filter time domain response')
subplot(2,1,2)
plot(fftshift(abs(fft(replica)))); %matched filter
frequency domain response
title('Matched filter frequency domain response')
for j = 1:1:nscat
t_tgt = 2. * (scat_range(j) - rmin) / c +htau;
x(j,1:uplimit) = scat_rcs(j) .* exp(i * 2.* pi * (.5 *
(b/taup) .* (t+t_tgt).^2));
y = y + x(j,:);
end
figure(2)
plot(t,real(y),'k') %plot of uncompressed echo signal
xlabel ('Relative delay - seconds')
ylabel ('Uncompressed echo')
title ('Zero delay coincide with minimum range')
rfft = fft(replica,nfft);
yfft = fft(y,nfft);
out= abs(ifft((rfft .* conj(yfft)) .* win' )) ./ (nfft);

```

A-3 Code for figure 5.4 & 5.5

```

clc
clear all
nscat=1; %Number of point scatterers within the received
window
rmin=150000; %Minimum range of receive window

```

```

rrec=200; %Receive window size
taup=.000005;%Uncompressed pulse width
f0=14e+6; %Chirp start frequency
b=16e+6;%Chirp bandwidth
scat_range=rmin+[0 25 50];%Vector of scatterers range
scat_rcs=[1 1 1]; %Vector of scatterers RCS
winid=0; %window function
eps = 1.0e-16;
htau = taup/2.;
c = 3.e8;
n = fix(2. * taup * b);
m = power_integer_2(n); %power_integer_2 calling function
nfft = 2.^m;
x(nscat,1:nfft) = 0.;
y(1:nfft) = 0.;
replica(1:nfft) = 0.;
if( winid == 0.)
win(1:nfft) = 1.;
win =win';
else
if(winid == 1.)
win = hamming(nfft); %hamming window function
else
if( winid == 2.)
win = kaiser(nfft,pi); %kaiser window function
else
if(winid == 3.)
win = chebwin(nfft,60); %chebwin window function
end
end
end

```



```

end
end
deltar = c / 2. / b;
max_rrec = deltar * nfft / 2.;
maxr = max(scat_range) - rmin;
if(rrec > max_rrec | maxr >= rrec )
'Error. Receive window is too large; or scatterers fall
outside window'
break
end
trec = 2. * rrec / c;

deltat = taup / nfft;
t = 0: deltat:taup-eps;
uplimit = max(size(t));
replica(1:uplimit) = exp(i * 2.* pi * (.5 * (b/taup) .*
t.^2));
figure(4)
plot(real(replica))
title('Matched filter time domain response')
figure(3)
plot(fftshift(abs(fft(replica))));
title('Matched filter frequency domain response')
for j = 1:1:nscat
t_tgt = 2. * (scat_range(j) - rmin) / c +htau;
x(j,1:uplimit) = scat_rcs(j) .* exp(i * 2.* pi * (.5 *
(b/taup) .* (t+t_tgt).^2));
y = y + x(j,:);
end
figure(1)

```

```

plot(t,real(y),'k')
xlabel ('Relative delay - seconds')
ylabel ('Uncompressed echo')
title ('Zero delay coincide with minimum range')
rfft = fft(replica,nfft);
yfft = fft(y,nfft);
out= abs(ifft((rfft .* conj(yfft)) .* win' )) ./ (nfft);
figure(2)
time = -htau:deltat:htau-eps;
plot(time,out,'k')
xlabel ('Relative delay - seconds')
ylabel ('Compressed echo')
title ('Zero delay coincide with minimum range')
grid

```

A-4 Code for figure 5.6

```

clc
clear all
nscat=3; %Number of point scatterers within the received
window
rmin=150000; %Minimum range of receive window
rrec=200; %Receive window size
taup=.000005;%Uncompressed pulse width
f0=14e+6; %Chirp start frequency
b=16e+6;%Chirp bandwidth
scat_range=rmin+[0 25 50];%Vector of scatterers range
scat_rcs=[1 1 1]; %Vector of scatterers RCS
win=0; %window function
eps = 1.0e-16;

```

```

htau = taup / 2.;
c = 3.e8; %speed of light
trec = 2. * rrec / c;
n = fix(2. * trec * b);
m = power_integer_2(n);
nfft = 2.^m;
x(nscat,1:nfft) = 0.;
y(1:nfft) = 0.;
if( win == 0.)
win(1:nfft) = 1.;
win =win';
else
if(win == 1.)
win = hamming(nfft); %hamming window function
else
if( win == 2.)
win = kaiser(nfft,pi); %kaiser window function
else
if(win == 3.)
win = chebwin(nfft,60); % chebwin window function
end
end
end
end
deltar = c / 2. / b;
max_rrec = deltar * nfft / 2.;
maxr = max(scatter_range) - rmin;
if(rrec > max_rrec | maxr >= rrec )
'Error. Receive window is too large; or scatterers fall
outside window'

```

```

break
end
deltat = taup / nfft;
t = 0: deltat:taup-eps;
uplimit = max(size(t));
for j = 1:1:nscat
psi1 = 4. * pi * scat_range(j) * f0 / c -4.* pi * b *
scat_range(j) * scat_range(j) / c / c/ taup;
psi2 = (4.*pi*b*scat_range(j) / c / taup) .* t;
x(j,1:uplimit) = scat_rcs(j).* exp(i * psi1 + i.*psi2);
y = y + x(j,:);
end
ywin = y .* win';
yfft = fft(y,nfft) ./ nfft;
out= fftshift(abs(yfft));
n1=rand(size(yfft));
out1=out+n1;
figure(2)
time = -htau:deltat:htau-eps;
plot(time,out)
xlabel ('Relative delay - seconds')
ylabel ('Compressed echo')
title ('Zero delay coincide with minimum range (without
noise)')
gridime = -htau:deltat:htau-eps;
grid

```

A-5 Code for figure 5.7

```
clc
```

```
clear all
b=1; %arbitrary constant
N=13; %barker code length
t=b/N*[1:1:(2*N-1)]; % compressed pulse width
x=[1 1 1 1 1 -1 -1 1 1 -1 1 -1 1]; %barker code
a=xcorr(x); %auto correlation of barker code
b=abs(a); %absolute value of auto correlated signal
plot(t, b); %plot of compressed pulse
```